

**The Journal of the Acoustical Society of America**  
**Extraterrestrial sound for planetaria: a pedagogical study**  
 --Manuscript Draft--

<b>Manuscript Number:</b>	JASA-00381R1
<b>Full Title:</b>	Extraterrestrial sound for planetaria: a pedagogical study
<b>Short Title:</b>	Extraterrestrial sound for planetaria
<b>Article Type:</b>	Special Issue Article
<b>Corresponding Author:</b>	Timothy G Leighton University of Southampton Southampton, Hampshire UNITED KINGDOM
<b>First Author:</b>	Timothy G Leighton
<b>Order of Authors:</b>	Timothy G Leighton Nikhil Banda Benoit Berges, PhD Phillip Joseph, PhD Paul White, PhD
<b>Section/Category:</b>	Physical Acoustics
<b>Keywords:</b>	Acoustics, planetary probes, Venus, Mars, Titan, thunder, dust devil, geyser, cryo-volcanoes, voice, auralisation, extra-terrestrial
<b>Abstract:</b>	The purpose of this project was to supply an acoustical simulation device to a local planetarium for use in live shows aimed at engaging and inspiring children in science and engineering. The device plays audio simulations of estimates of the sounds produced by natural phenomena to accompany audio-visual presentations and live shows about Venus, Mars and Titan. Amongst the simulated noise are the sounds of thunder, wind and cryo-volcanoes. The device can also modify the speech of the presenter (or audience member) in accordance with the underlying physics to reproduce those vocalisations as if they had been produced on the world under discussion. Given that no time series recordings exist of sounds from other worlds, these sounds had to be simulated. The goal was to ensure that the audio simulations were delivered in time for a planetarium's launch show to enable the requested outreach to children. The exercise has also allowed an explanation, in an age-appropriate way, of the science and engineering behind the creation of the sounds. This has been achieved for young children, and also for older students and undergraduates, who could then debate the limitations of that method, and how a fuller research programme might rectify them.

## 1 Extraterrestrial sound for planetaria: a pedagogical study

2

3 T. G. Leighton\*, N. Banda, B. Berges, P. F. Joseph, P. R. White

4

5 Institute of Sound and Vibration Research, University of Southampton, Highfield, Southampton SO17 1BJ,  
6 UK

7

8 \*Correspondence to: [tgl@soton.ac.uk](mailto:tgl@soton.ac.uk)

9

10 **Abstract:** The purpose of this project was to supply an acoustical simulation device to a local planetarium  
11 for use in live shows aimed at engaging and inspiring children in science and engineering. The device  
12 plays audio simulations of estimates of the sounds produced by natural phenomena to accompany audio-  
13 visual presentations and live shows about Venus, Mars and Titan. Amongst the simulated noise are the  
14 sounds of thunder, wind and cryo-volcanoes. The device can also modify the speech of the presenter (or  
15 audience member) in accordance with the underlying physics to reproduce those vocalisations as if they  
16 had been produced on the world under discussion. Given that no time series recordings exist of sounds  
17 from other worlds, these sounds had to be simulated. The goal was to ensure that the audio simulations  
18 were delivered in time for a planetarium's launch show to enable the requested outreach to children. The  
19 exercise has also allowed an explanation, in an age-appropriate way, of the science and engineering behind  
20 the creation of the sounds. This has been achieved for young children, and also for older students and  
21 undergraduates, who could then debate the limitations of that method, and how a fuller research  
22 programme might rectify them.

23

24

25 **Keywords:** Acoustics, planetary probes, Venus, Mars, Titan, thunder, dust devil, geyser, cryo-volcanoes,  
26 voice, auralisation, extra-terrestrial

27

28 PACS: 43.10.Sv, 43.20.Hq, 43.28.Dm, 43.28.Fp,

29

30

## I. INTRODUCTION

31

32 Broadly speaking there are two roles that acoustics plays in astronomy. The first is the auralisation of time  
33 series from astronomical measurements that may or may not be acoustic. The second is the use of acoustics  
34 to study oscillatory mechanical waves in the type of extra-terrestrial bodies that can support them. These  
35 bodies include dust clouds, suns etc., and this paper addresses sound in, or on, planetary bodies or moons.  
36 Collectively these studies are sometimes referred to as “sound in space”. The auralisation process may  
37 involve transferring into audible signals previously non-acoustic time-series which occur in the vacuum or  
38 near-vacuum of space and which correspond to physical processes which do not represent pressure  
39 fluctuations. Their translation into an acoustic form is therefore entirely artificial, but useful as a means of  
40 experiencing the phenomenon in the familiar form of sound. One such example involves making audible  
41 recordings from the measured electromagnetic radiation signal from a pulsar [1]. The goal of such  
42 rendering is to facilitate a greater understanding of the data, or to make the data more accessible to the non-  
43 expert. How non-acoustic signals are transferred to signals that may be experienced as sound relies upon  
44 how humans rely upon sound in the environment to convey information and may require, for example,  
45 frequency transposition in order to bring the signals into the audible frequency range. Such approaches are  
46 based upon converting a time-series, which may derive from complex unfamiliar objects, into the familiar  
47 and information-rich medium of sound. Conversely, the study of the acoustics on extra-terrestrial bodies is  
48 concerned with considering the physical properties of an environment and sources, and predicting (and  
49 eventually interpreting) the character of sounds as they may appear on those bodies.

50

51 The synthesis of sounds from non-acoustic phenomena has been considered for a variety of astronomical  
52 applications. Auralisation has been used to represent electromagnetic signals such as lightning on Jupiter  
53 or Saturn [2], and the effect of a probe passing through the bow wave formed when solar emissions meet  
54 such a planet’s massive magnetic field [3]. It has also been used to create acoustic signals representing  
55 propagating density perturbations in dust clouds, nebulae, noctilucent clouds, planetary rings, comets etc.  
56 [4-9]. Such low frequency, large scale perturbations, provide important information about the formation of  
57 stars and planets and their identification [10-14]. Low frequency seismic and interface waves in stars and  
58 planetary bodies [15] could also be auralized if converted to audible acoustic waves (which usually  
59 involves upshifting in frequency).

60

61 This paper considers problems which are a subset of the second category of sounds in space: the study of  
62 sounds on extra-terrestrial worlds. Work in this category can be further subdivided into two sub-classes.  
63 One is the prediction of the acoustical properties associated with physical processes that occur on the  
64 world under study. The other is the simulation of Earth-based sounds to recreate how they might be heard  
65 on another world. Predictions of the acoustic emissions from naturally occurring physical processes offers  
66 the possibility of designing systems that exploit these sounds to better understand the environment.  
67 Furthermore, these models can be used to test hypotheses on, for example, the nature of the natural sound  
68 sources; or the models could be used in an inverse mode to estimate the physical parameters of the source  
69 or environment from some future measurement of the acoustic signatures. The source might be natural, or  
70 introduced by the mission to reduce the number of unknowns.

71  
72 Understanding the acoustic environment on a planetary body allows the design of active acoustic  
73 instruments for use in probes or satellites. The most notable examples of this were associated with the  
74 highly successful Cassini-Huygens mission to Saturn's moon, Titan. Two acoustic instruments were  
75 developed for use on this mission. One employed a series of acoustic pulses reflected from the ground in  
76 order to determine the height of the probe from the surface [16], and another instrument used acoustic  
77 pulses transmitted between source and sensors on the probe to measure the atmospheric sound speed  
78 during descent [17]. Future uses of sound range from the local (consideration of how the 'ears' on a  
79 Martian space suit might better be able to warn an astronaut walking downhill of a rockfall behind him/her  
80 if the suit microphones are placed on the boot, not the helmet [18]) to the global (using the time taken for  
81 man-made or naturally occurring signals to propagate completely around the vast under-ice oceans of  
82 moons of Saturn and Jupiter to infer those ocean temperatures [18]).

83  
84 The motivation of the work reported in this paper was to provide a method for simulating a range of audio  
85 signals of naturally occurring extra-terrestrial phenomenon to engage the public in astronomy and related  
86 subjects. Simulating the acoustic environment on distant worlds is one way to capture the imagination of  
87 the broader community and can be used in conjunction with more conventional presentations, such as  
88 those frequently employed in a planetarium. Indeed this project was the result of a requirement to augment  
89 an existing presentation in a local planetarium. An additional output was that simple physics lessons for  
90 public engagement and schools were developed. Two examples include the investigation of how everyday  
91 phenomenon would be transformed on others worlds, and (for the more engaged student) criticising the  
92 limitations of the methods of producing those estimations. Acoustical phenomena are particularly useful

93 for this purpose since humans have evolved to appreciate even the slightest nuances in sound, and because  
94 in some ways alien atmospheres can affect sound far more than, say, light, generating very significant and  
95 counterintuitive effects. With this in mind, this study sets out to provide a local planetarium with the ability  
96 to provide audiences with the estimates of acoustical phenomena from other worlds, supported by  
97 explanations that can be expressed in terms of school-level physics. Essential for those undertaking such  
98 tasks is an appreciation that the project plan must take account of low budgets and short time-scales (as  
99 was the case here, with no budget and tight deadlines for a launch show).

100 For planetaria and film-makers, the current options of using Earth-based recordings of related phenomena,  
101 fictitious sounds or music, contrasts starkly with the integrity and detail available in the vast image  
102 libraries that can be readily accessed to portray planetary bodies.

103 In addition to public engagement and entertainment, there is another benefit to studying extra-terrestrial  
104 sound. It can reveal assumptions that have, over many years, been so well-validated from frequent  
105 application on Earth that they have become axiomatic. Testing them in extra-terrestrial environments can  
106 question that validation, improving instrument design and avoiding misinterpretations that can arise from  
107 the extra-terrestrial use of Earth-based intuition regarding sound and vibration. The use of common  
108 techniques for acoustic methods and definitions that are familiar practice on Earth can cause significant  
109 problems if applied to other worlds. Four examples are:

- 110 • First, the fluid loading that is often taken for granted in Earth-based calibrations of sensors and  
111 tests can be significantly different to that on Earth, depending on the geometry of the instrument  
112 and the atmosphere in which it is deployed [19];
- 113 • Second, although measurements of the sound speed is an established method of determining some  
114 characteristics of atmospheric chemistry [20] it has been found [21] that an established design  
115 would work during Earth-based tests but be potentially misleading on Venus or the gas giants (for  
116 where it has been proposed [20,22,23]). This indicates the extent to which engineering intuition  
117 informed by terrestrial experience must be questioned by examining the effect of the extra-  
118 terrestrial environments on the fundamental processes;
- 119 • Third, in coming decades the acoustical exploration of the vast under-ice water oceans, which  
120 dwarf those on Earth, found in some moons of the gas and ice giants will be considered. To do so  
121 we will also be required revisit the basic physics instead of relying on Earth-based engineering

122 intuition [18]. For example, the hydrostatic pressure in these oceans will be the major factor in  
123 determining how acoustic rays refract, just as it does on Earth where hydrostatic pressure is the  
124 major factor affecting sound propagation in the deep ocean. However, in predicting such ray paths  
125 in extra-terrestrial oceans, the expression for hydrostatic pressure should not be the  $\rho_w gh$  used by  
126 Earth ocean scientists and engineers (where  $\rho_w$  is the liquid density,  $g$  is the acceleration due to  
127 gravity, and  $h$  is the depth) [24,25].

128  
129 • Fourth, some terms in the sonar equations have become validated through decades of use in  
130 Earth's oceans and the atmosphere within (at most) a few miles of the ground, but the nature of  
131 those terms might require re-examination if inaccuracies are to be avoided when applying them to  
132 extra-terrestrial scenarios [26,27].

133 The focus of this paper will be on sounds in the three substantial ground-level extra-terrestrial atmospheres  
134 in our solar system, namely Venus, Mars and Titan, the properties of which are found in Petculescu and  
135 Lueptow [28] and Leighton and White [29]. Although other substantial atmospheres exist (such as on  
136 Jupiter and Saturn) and could be incorporated into an extended study of this sort, they were not done to  
137 ensure completion within a few months on no budget. Similarly, although sound exists in the solid and  
138 liquid components of other worlds, they are not included in this study. This is because the planetarium  
139 show was designed to teach about sound by exploiting the audience's familiarity with Earth-based sounds  
140 in air, comparing and contrasting these sounds with the extra-terrestrial ones. The audience would have had  
141 little experience with sounds in liquids and solids against which to benchmark the signals we produced for  
142 the planetarium, and therefore the choice was made to focus the effort on sounds in gases.

143 There are two types of prediction undertaken for this planetarium study: naturally occurring sounds and the  
144 human voice. This paper focuses on some of the naturally-occurring sounds that microphones of the future  
145 could potentially detect, focusing on volcanoes, thunder, dust devils and cryo-volcanoes. We simulated  
146 some of these sounds from the basic physics. However, in those cases where such simulations cannot even  
147 be made to produce a realistic Earth-like simulation of sound when Earth's environmental parameters are  
148 used as input, then recordings of the equivalent sound on Earth are transmuted to adapt for the extra-  
149 terrestrial parameters. Therefore whilst the sound of thunder, dust devils, and a methanefall can be entirely  
150 simulated, the sound of cryo-volcanoes [30] is produced by transmuting a sound recorded on Earth (as is  
151 that of a Titan probe's splashdown into a methane lake, though that is not detailed in this paper [31]). This  
152 paper indicates where each simulation lies in the scale between a rigorous untested prediction, and a clip  
153 provided simply for entertainment in the absence of any competing clips.

154 Whilst the sound files produced for the above phenomena could conceivably be validated within the  
155 foreseeable future, the second type of prediction is entirely fictional, and that is the human voice. However,  
156 voice simulations are undertaken for two reasons. The first is to provide the planetarium with a way of  
157 engaging with the public, since the human ear is extremely well attuned to changes in the human voice,  
158 perhaps more than to any other sound. Moreover, the public is engaged simply because the speech on any of  
159 these worlds is unobtainable. The simulations undertaken here change the voice because of changes in sound  
160 speed and fluid loading, two separate effects that give rise to different anthropomorphic impressions (the size  
161 of the speaker and the pitch of the voice) [32,33]. In addition to entertainment, there is a further public  
162 engagement aspect of all these simulations. Most of the science stories in the media concern confirmed results,  
163 so that the public does not for the most part see the scenario in which scientists find themselves for most of  
164 their projects, between making a prediction from theory and waiting to see the extent to which measurements  
165 conflict with theory and require it to be amended, adapted, or replaced. The necessity of sending a probe to  
166 another world to make these observations produces a tangible barrier between the moment the prediction is  
167 published, and the point at which these simulations are tested against observation. This creates a sustained  
168 period in which the public, like the scientists, can criticise the approach and speculate on what must be done to  
169 increase the chances of making observations that are sufficiently good to discern the accurate predictions from  
170 the inaccurate. Supplementary data files for these studies are available via the link in the Acknowledgements.

171

## 172 **II. BACKGROUND**

### 173 **A. Thunder**

174

175 Terrestrial thunder is the pressure pulse produced when an atmospheric lightning charge causes a rapid  
176 expansion of atmospheric gas, initiated by the sudden outwards thermal expansion (into the surrounding  
177 near-stationary cooler air) of the plasma in the lightning channel [34]. However, the character of the sound  
178 produced (a crack, a rumble etc.) depends both on the shape of that electrical discharge (straight, forked,  
179 sheet etc.) and features that affect propagation (ground and atmospheric characteristics, and range). The  
180 unrepresentative straight-line lightning channel assumed in the early simulations [35,36] produced a single  
181 short thunder clap. Low frequency rumble was only added [37] when the channel geometry was made  
182 jagged [38]. In this paper, only the lightning between the atmosphere and ground on is studied.

183

184 Atmospheric lightning on Venus (Fig. 1a) is thought to occur at around half the rate seen on Earth. Its  
185 presence has been inferred from whistler-mode waves [39] following initial attribution of EM bursts by the  
186 Soviet Venera probes [40]. Although ground level wind velocities are low (1 m/s) in the hot (740 K), dense  
187 atmosphere (which has a ground level pressure of 9.3 MPa and density of 67 kg/m<sup>3</sup>, i.e. 6.5% that of liquid  
188 water on Earth) [41], at higher altitudes in Venus' complex atmosphere, windspeeds can exceed 100 m/s  
189 (600% of the speed of planetary rotation, compared to ~20% seen for the fastest winds on Earth). The  
190 atmosphere is predominantly composed of carbon dioxide and the cloud content is dominated by sulphuric  
191 acid.

192  
193 Mars does not have liquid-bearing clouds and so it does not have thunder storms, and therefore the  
194 lightning is assumed to occur because of the build-up of charge in dust devils (Fig. 1b). This thermally-  
195 generated whirlwind, the lower part of which is made visible by the dust it raises, is a wholly separate  
196 phenomenon from a tornado. It is generated when solar heating of the ground causes hot air to rise up  
197 outside of the spinning column, while cooler air descends through its middle [42]. Charge distributions,  
198 like velocity profiles, are mutually dependent on the size and height of particles in the dust devil. Lightning  
199 is most likely from the larger dust devils (which tend to be less common than smaller ones), because the  
200 higher speeds within these can lift the heavier dust particles from the surface of Mars [43]. All dust devils  
201 were found to have low frequency electromagnetic emissions, which may be used to detect their presence,  
202 location and velocity [44].

203

## 204 **B. Dust devils**

205

206 In addition to the possible generation of acoustic signals due to lightning, Martian dust devils would also  
207 generate pressure signals associated with pressure fluctuations due to convected turbulence. Measurements  
208 of the coherence function between closely spaced microphone signals would be useful to assess the relative  
209 contribution of acoustic and hydrodynamic signals, which tend to be coherent over much shorter distances  
210 than acoustic pressure fluctuations.

211

212 Solar radiation heats the ground, causing atmosphere near it to rise through the cooler air above it, which is  
213 at lower pressure. Thinning of the rising column causes mass to move towards the axis, generating strong  
214 spin through conservation of angular momentum, which is intensified as warmer ground-level air is drawn  
215 into the base of the dust devil.

216

217 When fully developed, the shape of a dust devil consists on an inverted cone. The flow around and within a  
218 dust devil is divided into several regions [42, 45]: (i) The ‘outer region’ occurs around the dust devil, just  
219 outside the vortex core, and several meters above the surface. The flow in this area is governed by the  
220 vorticity of the core of the dust devil and the buoyancy in the convective current. (ii) The ‘corner region’ is  
221 called the ‘Ejecta skirt’ [45], within which particles are elevated into the main dust core. It contains the  
222 largest of the elevated particles. (iii) The ‘core region’ forms the main body of the dust devil, though lower  
223 particle loads mean it is less visible than the Ejecta skirt. (iv) The ‘near-surface layer region’ provides  
224 inflow to the corner region. (v) The ‘thermal plume region’ can extend hundreds of meters above the core  
225 region, and is barely visible because relatively low numbers of small particles resist gravity to reach the  
226 highest parts.

227  
228 One might consider designing acoustical detectors for probes, both for proximity warning and to open up  
229 the possibility of inversion of the emitted sound to measure dust devil parameters. To make such acoustical  
230 predictions, the mechanisms of sound production are quantitatively assessed using scaling laws derived by  
231 Morfey [46] to predict the sound power radiated to the far field, which are then corrected for atmospheric  
232 absorption. An energy spectrum is applied to this pressure field in order to obtain the frequency  
233 dependence. The resulting technique could predict the sound detected at a given range from a dust devil of  
234 a given size on Mars, having characteristics that change with the season and latitude.

235

### 236 **C. Cryo-volcanoes**

237

238 There is evidence suggesting the possible presence of cryo-volcanoes on Neptune’s moon Triton, Jupiter’s  
239 moons Io and Europa, and Saturn’s moons Titan and Enceladus [47-49]. Cryo-volcanos may contribute to  
240 the high hydrocarbon content of Titan’s atmosphere and surface [50,51], the hazy atmosphere of which  
241 would otherwise be depleted of hydrocarbon gases by sunlight through the photolysis that contributes to its  
242 characteristic haze and cloud cover. Unlike terrestrial volcanoes, which eject magma at high temperatures,  
243 cryo-volcanoes are cooler and release water, containing minerals, hydrocarbons (such as methane) and  
244 ammonia (although on Titan the liquid content is probably dominated by hydrocarbons [52]). The presence  
245 of liquid water in the moons of Saturn and Jupiter suggest heating by tidal forces, and in such  
246 circumstances pressurized water pockets can be generated and released to the surface (a solar heating  
247 model has also been proposed for Triton [53]). In many ways, cryo-volcanoes/geysers on Titan resemble  
248 terrestrial geysers [52]. Figure 1c shows a false colour 3D image from NASA’s Cassini spacecraft over an  
249 area of Titan, now known as Sotra Facula [30]. Topography and surface composition data enabled NASA  
250 scientists to suggest this as evidence for the existence of a possible extra-terrestrial cryo-volcano on Titan.

251

252 The objective in this paper is to provide details sufficient for schools to build their own model geysers or  
253 cryo-volcanoes and so stimulate discussion, rather than to duplicate any proposed mechanism by which a  
254 cryo-volcano might operate. The model here resembles a geyser, and significant heating is externally  
255 applied to generate the overpressure required for an eruption.

256

257

### 258 **III. METHODS**

259

260 The method by which the system for modifying speech is implemented has been described in detail  
261 previously [32,33]. The methods for generating the sounds of methanefalls and splashdowns on Titan have  
262 also been detailed elsewhere [29] with a later correction for the amplitude of excitation of bubbles [54].  
263 The sounds of voices and splashdowns used Earth-based recordings as their basis. The sounds of thunder,  
264 dust devils, and methanefalls were wholly simulated. The levels of rigor in deriving the sounds of dust  
265 devils and thunder were similar to those reported earlier for voices and methanefalls, commensurate with  
266 delivering only a first order study to produce a working device in short time scales. The sound of a cryo-  
267 volcano was less rigorous, being wholly contrived by building a physical model of a geyser. However, its  
268 inclusion was for a different purpose, specifically:

269

- 270 • To provide details sufficient for a physical working model to be constructed from these schematics  
271 by schools themselves;
- 272
- 273 • To stimulate discussion of whether or not an atmosphere of some sort is needed in order to generate,  
274 propagate and detect sound in places other than our own planet.

275

#### 276 **A. Thunder**

277

278 Following Hill's [38] method for simulating realistic lightning paths with characteristic zig-zag profiles,  
279 spark sound sources were divided into line segments of given length and each segment was aligned at a  
280 random angle to the previous segment. The angles of inclination were selected from a random distribution  
281 (with a bias towards vertical axis to generate realistic shape of lightning bolt in the manner used by Ribner  
282 and Roy [37]). Each line segment is then considered to be a source of sound. Using this approach, various  
283 lightning profiles can be simulated, two of which are shown in Fig. 2a to strike the same point on the  
284 ground (which, in the case of Martian lightning, might be the lower intake zone of the dust devil). In this

285 example, the longer lightning bolt is 1.8 km high and the shorter bolt is almost half its size at 850 m. The  
286 maximum size of the dust devils which might produce lightning bolts are believed to be 2 km to 8 km high.  
287 Figure 2 therefore represents lightning bolts occurring in a medium-to-large dust devil with multiple  
288 electrical discharges.

289  
290 In the absence of data on the lightning acoustic source strength on each planet, and because the  
291 atmospheric density and sound speed vary from site to site (making use of acoustic pressure problematic  
292 when comparing between planets [26]), it was decided that each 3 cm line segment would generate an N-  
293 wave that had the same intensity 1 m from the centre of the 3 cm segment (assuming spherical  
294 propagation). That intensity was  $1 \text{ pW m}^{-2}$ , chosen (i) to be small enough to ensure that acoustic pressure  
295 amplitudes do not become unfeasibly large in the thin Martian atmosphere, and (ii) for convenience, since  
296 the reference dB level for the lightning signals (perceived by an observer on the ground 1 km from the  
297 point where the lightning struck that ground) will be presented in dB relative to  $1 \text{ pW m}^{-2}$  (in compliance with  
298 international conventions [55]). Consequently the outputs only serve to show the different absorbing  
299 features of the atmosphere, since only the absorbance and sound speed of the atmospheres (and the  
300 attenuation from spherical spreading, which is similar on all planets and so invisible when comparing  
301 them) affect the signal [28]. The N-waves are modelled as initiating 1 m from the acoustic centre of the  
302 source [38], rather than by nonlinear propagation in the atmosphere [56]. The signal at 1 km on flat ground  
303 from the point of strike was very simply calculated, by assuming independent straight-line linear  
304 propagation path from each 3 cm segment to the observer, through an atmosphere where the sound speed  
305 does not vary with height or frequency along the propagation path (Earth=340 m/s; Venus=410 m/s;  
306 Mars=240 m/s; Titan=210 m/s) and neither does the density (Earth= $1.2 \text{ kg m}^{-3}$ ; Venus= $65 \text{ kg m}^{-3}$ ;  
307 Mars= $0.02 \text{ kg m}^{-3}$ ; Titan= $5.5 \text{ kg m}^{-3}$ ;) (Fig. 2b). The signals from the separate 3 cm segments are linearly  
308 superimposed at the observer [37].

309  
310 There are several important effects that are not included. The sound received at distance from the strike can  
311 be affected by the ground reflections, and the variation of atmospheric sound speed and absorption with  
312 frequency and height [28]. Upwardly-refracting atmospheres mean that sound emitted from the lightning  
313 channel above a certain height may not reach the observer on the ground. This can happen in cloud-to-  
314 cloud discharge when the lightning bolt is high in Earth's atmosphere. However, the low frequency  
315 acoustic components from cloud-to-ground discharges on Earth can usually be heard if the observer is less  
316 than 25 km away [34]. For Mars and Venus, Petculescu and Lupetow [28] observed that at the altitudes  
317 (below 8 km) and ranges (1-2 km) of interest, the sound speed over both the planets varies by only

318 between 3 and 7 m/s, causing only small perturbations from straight-line propagation, and there is now  
 319 increasing interest in the sound of lightning on Titan [57-59].

320  
 321 Even though Mars has a thin atmosphere, for the low altitudes under consideration here a continuum  
 322 approach is assumed to hold [60]. The method does require that each N-wave be represented as a pressure  
 323 signal 1 m from the centre of its 3 cm- long source element, and obtaining the amplitude of this wave from  
 324 the stated 1 pW m<sup>-2</sup> intensity requires use of an assumed sound speed and atmospheric density for each  
 325 planet. The method is made robust against details of the exact choice (because such exactitudes can be  
 326 problematic [26,27]) by ensuring that the reconstructed pressure time history at the observer is converted  
 327 back to intensity using the same assumed sound speeds and densities. If we had not used the artifice that  
 328 sound speed and density are constant along the propagation path, we would have opened up the question of  
 329 what standard values to choose for each planet, and whether to convert using such a standard value or using  
 330 the specific (and possibly different) values at range 1 m from the source and at the observer. The total  
 331 acoustic pressure time series at the observer may be obtained by summing the pressures from the  $n^{\text{th}}$  N-  
 332 wave segment of length  $l$ , assuming spherical spreading and including retarded time, as sketched in Fig. 2b,

$$333 \quad p(r, t) = A \int_{-l}^l \frac{N(ct - r_n)}{r_n} ds \quad (1)$$

334  
 335  
 336  
 337 where  $c$  is the local speed of the sound,  $N()$  is the time variation of the non-dimensional source strength of  
 338 the waveform of the N-wave, which has scaling amplitude  $A$  (in Pascals). The N-wave has duration,  $2T$ ,  
 339 which relates to the energy released per unit length in the lightning discharge, and here is set to 5 ms. The  
 340 lightning channel presented in the Fig. 2a is used in Eq. (1) for the simulation of thunder noise on Venus,  
 341 Mars and Titan. Different realisations of the profile in Fig. 2a are computed, based on a random number  
 342 generator to generate the angles between adjacent segments. The computations were performed to generate  
 343 a signal at a sampling frequency of 44.1 kHz. Once a pressure time series from the lightning event had  
 344 been constructed at the observer using this method, it was converted to a spectrogram of intensity using the  
 345 stated atmospheric sound speed and density, and then converted to dB using a 1 pW m<sup>-2</sup> reference.

346

## 347 **B. Dust devils**

348

### 349 *1. Sources in a dust devil*

350

351 Noise from dust devils is likely to arise from three principal aerodynamic generation mechanisms: (i)  
 352 Infasonic emissions, typically a few Hz, caused by low frequency oscillations of the entire rotating flow  
 353 system (Abdullah [61] has derived expressions for the first two natural frequencies of the vibrational  
 354 modes of the system, related to the tangential wind speed of the core, and the core radius); (ii) The  
 355 generation of volumetric quadrupole sources arising from the fluctuating shear stress generated by  
 356 turbulent mixing; (iii) Sound generation by the acceleration of density inhomogeneities.

357  
 358 The dominant noise source mechanism (i) is inaudible and will not be considered here for a planetarium  
 359 display. Mechanism (ii) is associated with one of the highest scaling laws observed in nature. Following  
 360 Lighthill [62], the radiated noise power from turbulent mixing noise varies as the eighth power of mean  
 361 flow speed. However, on both Earth and Mars, dust devil flows are restricted to low Mach numbers ( $U/c_0$ ,  
 362 where  $U$  is the local flow velocity and  $c_0$  the sound speed for linear waves) and this is not the dominant  
 363 source of sound.

364  
 365 In this paper we focus on the audible impression produced by mechanism (iii), although a future detector  
 366 microphone might make significant use of (i). The sound produced by flow inhomogeneities at low flow  
 367 speeds can be predicted to within an order of magnitude using the scaling laws developed by, for example,  
 368 Morfey [63]. That is to say, the density inhomogeneities of mass density  $\rho_s$  moving at a flow speed with  
 369 mean velocity  $U$  distributed over a volume  $\Delta V$  radiates at a distance  $r$  to a far field observer as:

370  

$$\overline{p^2} = \left(\frac{L}{r}\right)^2 \left(\frac{\rho_0 \rho_s}{c_0}\right)^2 U^6 \Delta V . \quad (2)$$
 371  
 372

373 However, the expression for overall mean square above provides no insight into the noise spectrum. For simplicity,  
 374 we assume that:

375  

$$\overline{p^2}(f) = \overline{p^2} \Phi(f) , \quad (3)$$
 376  
 377

378 where  $\Phi(f)$  is identical to the non-dimensional, normalised frequency spectrum for isotropic homogeneous  
 379 turbulence with integral length scale  $L$ , given by:

380  

$$\Phi(f) = \frac{4}{U} \frac{L}{1 + (2\pi fL/U)^2} , \quad (4)$$
 381  
 382

383 which has the normalisation property:

384

$$\int_0^{\infty} \Phi(f) df = 1 \quad (5)$$

385

386

387 The frequency spectrum of Eq. (5) has the characteristics of a low-pass filter with a cut-off frequency  
388 approximately equal to  $2\pi fL/U = 1$ . If we assume that the length-scale  $L$  scales with the dimensions of  
389 the dust devil itself, i.e.,  $L$ , then most of the noise is at very low frequencies, typically tens of Hz.

390

391 Overall noise from the dust devil can be predicted by summing the mean squared pressure from elementary  
392 volume contributions  $dV$  corresponding to regions between the ranges  $r$  and  $r + dr$ , the angles  $\phi$  and  
393  $\phi + d\phi$  and height  $z$  and  $z + dz$ , and there  $dV = dr r d\phi dz$  (Fig. 3a). Finally, effects of atmospheric  
394 absorption on sound attenuation is added, following published theory [28, 64-66].

395

396 The simple theory outlined above suggests that a simple prediction of the noise spectrum from a dust devil  
397 requires knowledge of the distribution of mean velocity, mass density and turbulence length-scale  
398 throughout the volume of the dust devil. It was implemented assuming a ground-level sound speed  
399 somewhat further from the equator than that typical for the lightning of the previous section (220 m/s) and  
400 absorption as given by Petculescu and Lueptow [28].

401

402 A dust devil is characterized by three regions: the radial inflow region, the core region and the thermal  
403 plume region. The radial inflow at the bottom of the dust devil corresponds to a very high vorticity region  
404 and the radial, tangential and vertical velocities are higher in this region. This is represented by a quadratic  
405 increase and decrease with a peak at the middle of this region. Outside the inflow region, the velocity is  
406 defined by a slight linear decrease with altitude. This flow speed variation is illustrated in Fig. 3b showing  
407 the behaviour of velocity components versus height  $z$ .

408

409

## 410 2. *Calculation of input parameters*

411

412 The mean flow speed variation in a typical dust devil was constructed from the literature [45, 67, 68],  
413 modelling the velocity profile in all three directions. Here we only summarise the main conclusions [66].  
414 The tangential velocity profile of dust devils approximates to a Rankine profile. In this, the tangential  
415 velocity in the main core of radius  $R_{\text{core}}$  is proportional to the radius, while the tangential velocity decreases

416 as the inverse of the radius in the outer region of the vortex of radius  $R_{\text{vortex}}$ . The vertical velocity profile  
417 versus the radius has been predicted by numerical simulations of dust devils from Large Eddy Simulations  
418 (LES) by Zhao *et al.* [42]. It is characterised by an increase in velocity from the center to the end of the  
419 vortex core and then a decrease with distance. Finally, the horizontal profile of the radial velocity is  
420 described by Balme and Greeley [43] and simulated by Zhao *et al.* [42]. Both predictions indicate zero  
421 velocity inside the vortex core followed by an increase until a maximum value and then a decrease beyond  
422 that.

423  
424

### 425 **3. Density profile**

426

427 The density profile required for the noise prediction is determined from the diameter of the particles inside  
428 the dust devil and the particle density. Following Jackson *et al.* [69], a constant number density of the  
429 order of  $10^8$  grains/m<sup>3</sup> was assumed for this simplified model of a Martian dust devil. The ability of the  
430 flow to lift dust and sand particles is related to the updraft speed of the dust devil. Grain diameters are  
431 calculated from the threshold ‘lifting’ wind velocity [70] at which particles start moving in response to the  
432 action of the wind (each grain has a mineral density of 3000 kg m<sup>-3</sup>). In the simulations here, the particle  
433 diameter and density profiles used are plotted as a function of the vertical speed in Fig. 4. The following  
434 representative values are assumed for the dust devil: the height of the dust devil  $h = 250$  m; the maximum  
435 radius of the core region of the dust devil  $R_{\text{core}} = 50$  m; the maximum radius of the vortex region of the  
436 dust devil  $R_{\text{vortex}} = 70$  m; the length scale of the dust devil  $L = R_{\text{vortex}}/100$ , used when defining the  
437 frequency dependence of the acoustic pressure field [71]. The initial, peak and maximum mean velocities  
438 assumed in the simulations in the tangential direction  $v$  are (30, 35, 25) m/s, in the vertical direction  $w$  (20,  
439 25, 15) m/s and in the radial direction  $u$ , (7, 5, 4) m/s, respectively.

440  
441

442  
443

### 444 **C. Cryo-volcanoes**

445

446 Figure 5 shows a schematic of the apparatus which models a terrestrial geyser (based on one built around  
447 1977 by one of the authors [see Acknowledgements], and independently rediscovered more recently  
448 [72,73]). A flask of water (the ‘deep reservoir’) is continually heated, the only outlet being a long pipe that  
449 opens at the top to a ‘lake’ (safely enclosed in the current version, but open to the lab in a ‘funnel’ crater in  
450 the 1977 apparatus and in Lasic’s version [73]). In the ‘lake’ the water temperature is cooler. The

451 following description enters the cycle just after an eruption, when cooler water from the lake has  
452 descended the tube into the deep reservoir. As the temperature in the water at the base rises, gas comes out  
453 of solution: it had previously dissolved into the cooler lake water when it was open to the atmosphere (this  
454 of course invites discussion with undergraduates on how this apparatus compares to a cryo-volcano, and  
455 the role of static pressure and temperature, phase changes and vapor).

456  
457 Depending on the temperature and the static pressure (which may be very low close to the surface if there  
458 is no atmosphere) at key locations, boiling can occur. Water travels up the riser tube through a number of  
459 mechanisms: although thermal expansion does occur, level rise in the ‘lake’ is dominated by the rise of any  
460 gas plugs and other bubbles up the pipe. This produces the gradual rise in lake level seen in terrestrial  
461 geysers before eruption. A key factor is the pressure in the deep reservoir, which see a steady reduction if  
462 bubbles lift the water column above them, and also sees transient pressure changes as bubbles reach the  
463 lake prior to eruption: this can generate some splashing. Explosive eruption occurs because, whilst heat is  
464 being supplied to the base making it hotter, the pressure on the deep reservoir from the column of liquid is  
465 being reduced by the bubbles, lowering the boiling point in the flask. At a critical point, the rising  
466 temperature and reducing pressure pass a rapid transition to boiling phase, which causes mass and energy  
467 to travel from the deep reservoir to the lake. This persists until the eruption can no longer be sustained.  
468 Cooler water from the lake then travels down the riser tube to the deep reservoir (replenishing the reservoir  
469 with dissolved gas if the lake is open to the atmosphere), with commensurate condensation as cooling  
470 occurs, and the cycle begins again.

471  
472 There is a layer of detail in the theory for the eruptions (including the roles of constrictions in the pipe,  
473 surface tension changes in the liquid, bubble traps etc. [52, 74, 75]) that go into greater depth than this  
474 simple demonstration warrants (although limitations relating to the local sound speed, which are usually  
475 not important on Earth, have been proposed for other worlds [76]). In this paper, two types of geyser will  
476 be produced, one that erupts at regular intervals, and one that does not erupt but delivers liquid and bubbles  
477 to the surface of the world or moon.

478 Figure 5 shows two versions of the apparatus that were built. Each contained 500 ml of water (when filled  
479 to generate a ‘boiling’ geyser – see section IIIC), and a PMMA safety shield contains the apparatus (which  
480 sits over an empty tank that can catch the water in case of breakage or leakage – not shown in Fig. 5). An  
481 electrical heater (Barnstead International 150 W) with a protective circuit breaker, was used. Depending on  
482 the availability of equipment, hydrophones (Bruel and Kjaer 8103) and thermocouples were deployed in  
483 the lake and the deep reservoir, a microphone was set up in air by the lake (PCB ICP426E01), a video

484 camera recorded the water level in the lake, and accelerometers (type 352C22) were placed on the flask  
485 containing the lake (which was spherical for safety in (a), but replaced in (b) by a conical ‘crater-like’ one  
486 resembling that used in the 1977 original). Use of more sensors to map the signals at various locations and  
487 ranges was prevented by budget constraints, but would be desirable. Indeed, the use of a single microphone  
488 on a planetary probe does not allow identification of the source of pressure fluctuations on that microphone  
489 [77], i.e. whether they are truly acoustic (in that acoustical energy propagates to distance), or whether they  
490 are hydrodynamic or aerodynamic pressure fluctuations at source (or convected from some nearby source)  
491 that do not therefore represent the soundscape of that world, and should not be represented as such.

492

### 493 **III RESULTS**

494

#### 495 **A. Thunder**

496

497 Figure 6 plots the intensity spectrograms recorded on flat ground 1 km away from the point where  
498 lightning strikes the ground, with no refraction or ground effects included. Because each 3 cm emits an  
499 identical N-wave of intensity  $1 \text{ pW m}^{-2}$  at 1 m from the acoustic centre of the element, the dB levels (re  $1$   
500  $\text{pW m}^{-2}$ ) in Fig. 6 reflect the effects of atmospheric absorption [28]. Figure 6a shows the baseline, the  
501 thunder for the sound speed of Earth, but without any atmospheric absorption. Losses in Fig. 6a are due  
502 to spherical spreading only: this will be similar on all worlds, so for the most part is invisible when  
503 comparing the four graphs. The sound speed on Mars is low [28], which would give a long detected signal  
504 except that the absorption on Mars is the highest of the planets studied here, and so does not allow the  
505 detected signal to persist (Fig. 6b). Venus has the highest sound speed, so would have the shortest signal if  
506 no absorption were taken into account, although the received signal is dominated by the fact that at  
507 frequencies above around 100 Hz its absorption is substantially greater than that of Earth’s atmosphere  
508 [28]. Titan has, by a substantial margin, the lowest sound speed and absorption, so that its thunder signal  
509 persists the longest and contains significant high frequency information.

510

#### 511 **B. Dust devils**

512

513 Figure 7 maps rms sound pressure level versus height and radial distance at four different frequencies: 500  
514 Hz, 2000 Hz, 3500 Hz and 5000 Hz. The sound pressure level decreases with frequency, range and height.  
515 The highest sound levels are observed at locations closest to the inflow region of the dust devil, where the  
516 vorticity is highest. Although these predictions are subject to considerable uncertainties because the main  
517 parameters of density, length-scale, dust devil dimensions and magnitude of the wind speed are themselves

518 poorly understood in this scenario, nevertheless this simple approach provides a first order prediction of  
519 the noise spectra that is useful for illustrative purposes in the planetarium.

520

### 521 **C. Cryo-volcanoes**

522

523 With the apparatus shown in Fig. 5, a range of phenomena could be generated by, for example, allowing  
524 flow into the deep reservoir via the return tube and from the cold reservoir (items shown in (b) but not  
525 present in (a), these flows being controllable by valves). The cold reservoir could be used to adjust the  
526 levels in the lake and provide different conditions or flow into the deep reservoir. The addition of anti-  
527 bumping granules to the deep reservoir would ensure that the boiling of water would be uniform to avoid  
528 any sudden superheated water to ‘shoot out’. However, from this range of possibilities, only two are  
529 reported in this paper: a ‘boiling’ and an ‘overflowing/shooting’ geyser. Other types of geyser (non-  
530 overflowing, pool, hot spring and steam vent [78]) were assessed as unsafe for use by students. Although  
531 spectacular results could be obtained without anti-bumping granules in the deep reservoir, for safety all  
532 student experiments used such granules.

533 Preliminary experiments were conducted with the apparatus shown in Fig. 5a. As the water temperature  
534 increases, previously dissolved gas comes out of solution, and small bubbles rise up the riser tube without  
535 significantly increasing the level of water in the lake. As the temperature increases, a rise in lake level (Fig.  
536 8a) heralds violent boiling in the deep reservoir at a temperature of approximately 104°C, in agreement  
537 with calculations based on the extra static pressure contribution caused by the hydrostatic head of the riser  
538 tube and lake. When boiling occurs in the deep reservoir, a large vapour/gas bubble rises into the channel  
539 without collapsing, followed by other bubbles. When these bubbles reach the surface, a slight eruption  
540 starts. It lasts for a few seconds (from 16 s to 21 s in Fig. 8b, as indicated by the record from a hydrophone  
541 placed 2 cm from the central axis of the upper flask) before there is insufficient pressure to prevent cooler  
542 water flowing back from the lake into the deep reservoir, such that the boiling stops. The drop of the water  
543 level in the upper flask is so great as to expose the hydrophone to air, so that it picks up no sound in the  
544 period 21-24 s (as shown by the movie in the supplementary material referenced from the  
545 Acknowledgements). Use of a lake with deeper pockets would prevent this artefact.

546 Figure 9 shows the measurement over two eruptions of the temperature in the deep reservoir (panels (a,c)),  
547 and the lake [panels (b,d)], with two different lake starting temperatures, ~50°C [panels (a,b)] and ~80°C  
548 [panels (c,d)]. The data are averaged over 10 runs. The deep reservoir temperature oscillates in the  
549 expected manner, rising until eruption occurs, a process which is followed by cooling and condensation as

550 cooler water flows from the lake to the deep reservoir. At lake temperatures below roughly 70°C, the lake  
551 temperature shows a gradual rise, on which are superimposed peaks during eruptions (Fig. 9b). This trend  
552 ceases when the lake temperature reaches around 78°C, at which point the lake temperature oscillates  
553 around this value as eruptions heat it temporarily. A gradual rise in lake temperatures will tend to shorten  
554 the time between eruptions, as the deep reservoir requires less time to attain the temperature required to  
555 boil (the minimum in Fig. 9a) is 97.5°C (and the time between eruptions is 125 s), several degrees cooler  
556 than the ~100°C minimum in Fig. 9c, when there is only 80 s between eruptions).

557  
558 Comparison of Fig. 9(c,d) most readily shows the steady state, where a steady temperature rise in the deep  
559 reservoir is followed by an eruption that warms the upper lake, after which water from the lake falls down  
560 the channel to cool the deep reservoir. A hydrophone in the lake (Fig. 9e) and an accelerometer on the  
561 outside of the upper flask (Fig. 9f), show eruption signals (the accelerometer not being prone to silence due  
562 to exposure in air which affects the hydrophone signal – see comments in caption to Fig. 8a). Whilst Fig.  
563 8a showed that the lake level rises prior to the eruption as bubbles draw water up the riser tube, and returns  
564 to its original form after the eruption, the temperature sensors show that some water from the deep  
565 reservoir remains, raising its temperature (Fig. 9b,d) and some lake water falls to the deep reservoir,  
566 cooling it (Fig. 9a,c).

567  
568 To generate time series suitable for use in our planetarium device, an in-air microphone was added outside  
569 the lake (3 cm from the water), a return feed was added from the lake to the deep reservoir, and the  
570 spherical container for the lake was replaced by a conical one. Unfortunately at this time the video camera,  
571 thermocouples and accelerometer were no longer available. A ‘boiling’ geyser was generated by filling  
572 the upper flask (containing the lake) with water to a depth of 10 cm from the base of the cone (the top of  
573 the riser tube). Once the cycle had been set up, it erupted every 356 s. A ‘shooting’ or ‘overflowing’ geyser  
574 was generated by keeping this flask empty, the water being filled to the top of the riser tube only. Prior to  
575 an eruption, it rose by 10 mm, at which time the water temperature in the lake reached 102°C. Once in  
576 steady state, it erupted every 240 s, because of the volume and head of water were less than before.

577  
578 The boiling geyser used the arrangement shown in Fig. 5b, with the valves on the return tube open. Whilst  
579 boiling is continuous in the deep reservoir, bubbles coalesce in the riser and are ejected only intermittently  
580 into the lake (with bubble sizes considerably larger than when they first enter the riser), which here is a  
581 reverberant environment (note that in a larger tube bubble dynamics will differ [79-81]). With the same  
582 experimental arrangement, but with the lake flask empty in order to generate a shooting geyser, the

583 microphone record is shown in Fig. 10a. The microphone record is far more noisy than the hydrophone  
584 records of Fig. 8 and 9, largely because of the in-air sound in the laboratory. The electric heater at the deep  
585 reservoir was turned off at time  $t=400$  s after the start of the recording, causing an almost immediate  
586 decrease in activity: whilst geothermal heat sources would not normally cease so suddenly, if intense  
587 differences in solar heating are a factor there will be such an effect, perhaps for example in ice comets. The  
588 Welch Power Spectral Density estimate is shown in the inset, and indicates no signal above background  
589 above 3 kHz.

590 After testing both boiling and shooting geysers for the planetarium show [82], the decision was made to  
591 use the in-air microphone recording of a shooting geyser as the basis for the planetarium show. This is  
592 because it served the purpose of requesting children in a show to imagine ‘what their ears might hear if  
593 they survived on Titan’ than did the hydrophone record. It contained both the noise from the lake and the  
594 sound from the boiling deep reservoir.

595 For the purposes of the planetarium exhibition, a 9 s segment (Fig. 10(b,c)) was generated from the  
596 shooting geyser record of Fig. 10(a). There is currently too little information definitively to choose one  
597 method of transposing the geyser sounds from Earth to Titan. Previously [54], the Minnaert equation had  
598 been transposed from Earth to Titan to generate the sound of the ‘methanefall’, on the assumption that the  
599 natural frequencies of the bubbles would dominate the sound. Having used this method once [54], an  
600 alternative approach was chosen for the geyser, to open up discussions with undergraduates on their  
601 relative merits and validities and differing outcomes. For the geyser therefore, with little supporting  
602 evidence, the transposition was made as if the sound were dominated by the physical scale of the structures  
603 in air (transposing frequencies by the ratio of the ground level atmospheric sound speeds on the two  
604 worlds). The structures in question would include the lake craters, and the craters of popping bubbles. The  
605 latter was chosen because of its pedagogical potential: It celebrates the century since Sir William Bragg  
606 [83], in the 1919 Royal Institution childrens’ Christmas lectures, suggested that the sounds emitted by  
607 running water originate from cavities created by the impact of liquid drops on the water surface. Bragg  
608 cited the (previously unpublished) work of Sir Richard Paget who modelled these cavities (as  
609 photographed in 1908 by Worthington [84]) out of plasticine and found that by blowing across openings in  
610 them sounds were produced similar to those heard when objects were dropped into water. Although  
611 replaced by the work of Minnaert as the established mechanism for bubble sounds, it was here (possibly  
612 erroneously) used to model a substantial contribution to the sounds of a Titan geyser.

613

#### 614 IV. PLANETARIUM FACILITY

615  
616 The algorithms described in this paper were interfaced with a Graphical User Interface (GUI) in a  
617 laptop and supplied to the Astrium Planetarium at INTECH, Winchester, UK (now Winchester Science  
618 Centre & Planetarium). Thunder on Mars, Venus and Titan, dust devil noise on Venus, the sound of cryo-  
619 volcanos on Titan, were included using the methods of this paper. The device also included the sounds of  
620 methanefalls on Titan, a Titan probe's splashdown into a methane lake, and a voice changer for Mars,  
621 Titan and Venus, which have been described elsewhere [29,31-33,54]. The first planetarium show  
622 featuring the device occurred on 4 April 2012 [85]. Since then it also featured in the 19th Dutch Annual  
623 Quiz [86] and in educational TV shows [87]. Given the short timescales and lack of funding, the results  
624 have generated considerable interactions with the public, including form of presentations, Q&A sessions  
625 and school visits etc. The validity of the simulations varies significantly, the assumptions and methods can  
626 readily be criticised and many could be improved upon. As such this work has facilitated considerable  
627 engagement with undergraduate- and Masters-level students who have become interested in an area in  
628 which they can see their suggestions are capable of improving upon what is currently offered in this  
629 emerging area of research.

630  
631 **Acknowledgments:** This work was unfunded. Mr Banda and Mr Berges completed their contributions to  
632 this study during their MSc projects, which were supervised by TGL, PRW and PFJ. The authors are  
633 grateful to Jenny Shipway and the staff of the Astrium Planetarium at INTECH, Winchester, UK. The  
634 authors are very grateful to Dr Andi Petculescu for many fruitful discussions over the years. TGL is  
635 grateful to his physics teacher, Mr Colin James of Heversham Grammar School, who in the 1970s  
636 constructed with him the first model geyser in order to test whether lake level rises preceded eruption,  
637 whether eruptions were associated with reduction in pressure as bubbles rose up the tube, and whether the  
638 timing between eruptions could be made regular and predictable. The data supporting this study, including  
639 time series, are openly available from the University of Southampton repository at  
640 <http://dx.doi.org/10.5258/SOTON/xxxxx>.

#### 641 642 **References**

- 643  

---

  
1 Jodrell Bank Centre for Astrophysics, "The sounds of pulsars," The University of Manchester,  
<http://www.jb.man.ac.uk/pulsar/Education/Sounds/> (2014) (date last viewed 31/01/16).

- 
- 2 Space Audio, "The Sounds of Lightning at Saturn," The University of IOWA, <http://www-pw.physics.uiowa.edu/space-audio/cassini/cas-sed-06-023-2hr/pw.physics.uiowa.edu/space-audio/cassini/cas-sed-06-023-2hr/> (2006) (date last viewed 31/01/16).
  - 3 Space Audio, "Cassini Encounters Saturn's Bow Shock," The University of IOWA. <http://wwwpw.physics.uiowa.edu/space-audio/cassini/bow-shock/> (2004) (date last viewed 31/01/16).
  - 4 F. Verheest, "Are weak dust-acoustic double layers adequately described by modified Korteweg-de Vries equations?" *Physica Scripta*, 47, 274-277 (1993).
  - 5 J. B. Pieper and J. Goree, "Dispersion of plasma dust acoustic waves in the strong-coupling regime," *Physical Review Letters*, 77, 3137-3140 (1996).
  - 6 M. Rosenberg and G. Kalman, "Dust acoustic waves in strongly coupled dusty plasmas," *Physical Review E*, 56, 7166-7173 (1997).
  - 7 R. L. Merlino, "current-driven dust ion acoustic instability in a collisional dusty plasma," *IEEE Transactions on Plasma Science*, 25, 60-65 (1997).
  - 8 P. K. Shukla, "Dust acoustic wave in a thermal dusty plasma," *Physical Review E*, 61, 7249- 7251 (2000).
  - 9 M. R. Gupta, S. Sarkar, S. Ghosh, M. Debnath and M. Khan, "Effect of nonadiabaticity of dust charge variation on dust acoustic waves: Generation of dust acoustic shock waves," *Physical Review E*, 63, 046406-1 - 046406-9 (2001).
  - 10 Y. Elsworth, R. Howe, G. R. Isaak, C. P. McLeod and R. New, "Variation of low-order acoustic solar oscillations over the solar cycle," *Nature* 345, 322-324 (1990).
  - 11 W. Rammacher and P. Ulmschneider, "Acoustic waves in the solar atmosphere. IX- Three minute pulsations driven by shock overtaking," *Astron. and Astrophys.* 253, 586-600 (1992)
  - 12 U. Lee, "Acoustic oscillations of Jupiter," *The Astrophysical Journal*, 405, 359-374 (1993).
  - 13 R. W. Noyes, S. Jha, S. G. Korzennik, M. Krockenberger, P. Nisenson and T. M. Brown, "A planet orbiting the star  $\rho$  Coronae Borealis," *The Astrophysical Journal*, 483, L111-L114 (1997).
  - 14 F. Bouchy, M. Bazot, N. C. Santos, S. Vauclair and D. Sosnowska, "Astero-seismology of the planet-hosting star  $\mu$  Arae. I. The acoustic spectrum," *Astronomy and Astrophysics*, 440, 609- 614 (2005).
  - 15 A. G. Kosovichev, "Properties of Flares-Generated Seismic Waves on the Sun", *Solar Physics* 238(1), 1-11 (2006) doi: 10.1007/s11207-006-0190-6.

- 
- 16 J. C. Zarnecki, M. R. Leese, B. Hathi, A. J. Ball, A. Hagermann, M. C. Towner, R. D. Lorenz, J. A. M. McDonnell, S. F. Green, M. R. Patel, T. J. Ringrose, P. D. Rosenberg, K. R. Atkinson, M. D. Paton, M. Banaszekiewicz, B. C. Clark, F. Ferri, M. Fulchignoni, N. A. L. Ghafoor, G. Kargl, H. Svedhem, J. Delderfield, M. Grande, D. J. Parker, P. G. Challenor and J. E. Geake, “A soft solid surface on Titan as revealed by the Huygens Surface Science Package,” *Nature* 438, 792795 (2005).
  - 17 J. P. Lebreton, O. Witasse, C. Sollazzo, T. Blancquaert, P. Couzin, A. –M. Schipper, J. B. Jones, D. L. Matson, L. I. Gurvits, D. H. Atkinson, B. Kazeminejad and M. Pérez-Ayúcar, “An overview of the descent and landing of the Huygens probe on Titan,” *Nature* 438, 758–764 (2005).
  - 18 T. G. Leighton, P. R. White and D. C. Finfer, “The opportunities and challenges in the use of extra-terrestrial acoustics in the exploration of the oceans of icy planetary bodies,” *Earth Moon and Planets*, 109 (1-4), 91-116 (2012) (doi:10.1007/s11038-012-9399-6).
  - 19 T. G. Leighton, “Fluid loading effects for acoustical sensors in the atmospheres of Mars, Venus, Titan and Jupiter,” *Journal of the Acoustical Society of America*, 125(5), EL214-EL219 (JASA Express Letters doi: 10.1121/1.3104628) (2009).
  - 20 R. A. Hanel, “Exploration of the atmosphere of Venus by a simple capsule,” NASA Technical Note TN D-1909 (1964).
  - 21 J. Jiang, K. Baik and T. G. Leighton, “Acoustic attenuation, phase and group velocities in liquid-filled pipes II: Simulation for spallation neutron sources and planetary exploration,” *Journal of the Acoustical Society of America*, 130(2), 695-706 (2011) (doi:10.1121/1.3598463).
  - 22 R. A. Hanel and M. G. Strange, “Acoustic experiment to determine the composition of an unknown planetary atmosphere,” *J. Acoust. Soc. Am.* 40, 896–905 (1966).
  - 23 D. Banfield, P. Gierasch, and R. Dissly, “Planetary descent probes: Polarization nephelometer and hydrogen ortho/para instruments,” *Proc. IEEE Aerosp. Conf.* 2005, 691–697 (2005).
  - 24 T. G. Leighton, D. C. Finfer and P. R. White, “The problems with acoustics on a small planet,” *Icarus*, 193(2), 649-652 (2008).
  - 25 T. G. Leighton, “The use of extra-terrestrial oceans to test ocean acoustics students,” *Journal of the Acoustical Society of America*, 131(3 Pt 2), 2551-2555 (2012) (doi: 10.1121/1.3680540)
  - 26 M. A. Ainslie and T. G. Leighton, “Sonar equations for planets and moons,” *Proceedings of the 22nd International Congress on Sound and Vibration. Major challenges in Acoustics, Noise and Vibration Research, 2015* (Edited by: Crocker MJ, Pawelczyk M, Pedrielli F, Carletti E, Luzzi S . ISSN 2329-3675, ISBN 978-88-88942-48-3). (Florence, Italy, 12016 July 2015) Paper number 1304 (8 pages) (2015).
  - 27 M. A. Ainslie, *Principles of sonar performance modeling*, Springer (2010) pp. 33, 493, 576, 607-610.

- 
- 28 A. Petculescu and R. M. Lueptow, "Atmospheric acoustics of Titan, Mars, Venus, and Earth," *Icarus*, 186, 413-419 (2007).
- 29 T. G. Leighton and P. R. White, "The Sound of Titan: A role for acoustics in space exploration," *Acoustics Bulletin*, 29(4), 16-23 (2004).
- 30 J.-R. Cook, D. C. Brown, P. Laustsen, "Cassini Spots Potential Ice Volcano on Saturn Moon," *Cassini Solstice Mission, News and Features* (Dec 14, 2010), Jet Propulsion Laboratory California Institute of Technology, <http://saturn.jpl.nasa.gov/news/newsreleases/newsrelease20101214/> (2010) (last observed 5 December, 2015).
- 31 T. G. Leighton and P. R. White, "The sounds of voices and waterfalls on other planets" [http://www.southampton.ac.uk/engineering/research/projects/the\\_sounds\\_of\\_voices\\_and\\_waterfalls\\_on\\_other\\_planets.page](http://www.southampton.ac.uk/engineering/research/projects/the_sounds_of_voices_and_waterfalls_on_other_planets.page) (last accessed 23 June 2016)
- 32 T. G. Leighton and A. Petculescu, "The sound of music and voices in space Part 1: Theory," *Acoustics Today*, 5(3), 17-26 (2009).
- 33 T. G. Leighton and A. Petculescu, "The sound of music and voices in space Part 2: Modeling and simulation," *Acoustics Today*, 5(3), 27-29 (2009).
- 34 V. A. Rakov and M. A. Uman. *Lightning: Physics and effects* (Cambridge University Press, Cambridge, 2007) 687 pages.
- 35 M. N. Plooster, "Numerical Model of the Return Stroke of the Lightning Discharge," *Phys. Fluids* 14, 2124-2133 (1971).
- 36 R. D. Hill, "Channel Heating in Return-Stroke Lightning," *J. Geophys. Res.* 76, 637-645 (1971).
- 37 H. S. Ribner and D. Roy, "Acoustics of thunder: A quasilinear model for tortuous lightning," *Journal of Acoustical Society of America*, 72(6), 1911-1925 (1982).
- 38 R. D. Hill, "Analysis of irregular paths of lightning channels," *J. Geophysical Research*, 73(6), 1897-1906 (1968).
- 39 C. T. Russell, T. L. Zhang, M. Delva, W. Magnes, R. J. Strangeway and H. Y. Wei, "Lightning on Venus inferred from whistler-mode waves in the ionosphere," *Nature*, 450 (7170): 661-662 (2007).
- 40 L. V. Ksanfomaliti, "Lightning in the cloud layer at Venus," *Kosm. Issled.*, 17, 747-762 (1979).
- 41 A. T. Basilevsky and J. W. Head, "The surface of Venus". *Rep. Prog. Phys.* 66 (10): 1699-1734 (2003) doi:10.1088/0034-4885/66/10/R04.
- 42 Y. Z. Zhao, Z. I. Gu, Y. Z. Yu, Y. Ge, Y. Li, X. Feng, "Mechanism and large eddy simulation of dust devils," *Atmosphere-Ocean*, Volume 42(1), 61-84 (2004)

- 
- 43 M. Balme and R. Greeley, "Dust devils on Earth and Mars," *Reviews of Geophysics*, 44(3), RG3003, 2006. doi: 10.1029/2005RG000188 (22 pages).
- 44 N. O. Renno, A.-S. Wong and S. K. Atreya, "Electrical discharges and broadband radio emission by Martian dust devils and dust storms," *Geophysical Research Letters*, 30(22), 2140 (2003) doi:10.1029/2003GL017879. (4 pages).
- 45 T. J. Ringrose, M. R. Patel, M. C. Towner, M. Balme, S. M. Metzger, J. C. Zarnecki, "The meteorological signatures of dust devils on Mars," *Planetary and Space Science*, 55, 2151-2163 (2007).
- 46 C. L. Morfey, "Amplification of aerodynamic noise by convected flow inhomogeneities," *J. Sound and Vibration*, 31(4), 391-397 (1973).
- 47 J. R. Spencer, J. C. Pearl, M. Segura, F. M. Flasar, A. Mamoutkine, P. Romani, B. J. Buratti, A. R. Hendrix, L. J. Spilker, R. M. C. Lopes, "Cassini Encounters Enceladus: Background and the Discovery of a South Polar Hot Spot," *Science*, 311, 1401-1405 (2006)
- 48 C. C. Porco, P. Helfenstein, P. C. Thomas, A. P. Ingersoll, J. Wisdom, R. West, G. Neukum, T. Denk, R. Wagner, T. Roatsch, S. Kie\_er, E. Turtle, A. McEwen, T. V. Johnson, J. Rathbun, J. Veverka, D. Wilson, J. Perry, J. Spitale, A. Brahic, J. A. Burns, A. D. DelGenio, L. Dones, C. D. Murray, S. Squyres, "Cassini Observes the Active South Pole of Enceladus *Science*," 311, 1393-1401 (2006).
- 49 S. Bargmann, R. Greve and P. Steinmann, "Simulation of cryo-volcanism on Saturn's moon Enceladus with the Green-Naghdi theory of thermoelasticity," *Bulletin of Glaciological Research*, 26, 23-32 (2008).
- 50 C. Sotin, R. Jaumann, B. J. Buratti, R. H. Brown, R. N. Clark, L. A. Soderblom, K. H. Baines, G. Bellucci, J.-P. Bibring, F. Capaccioni, P. Cerroni, M. Combes, A. Coradini, D. P. Cruikshank, P. Drossart, V. Formisano, Y. Langevin, D. L. Matson, T. B. McCord, R. M. Nelson, P. D. Nicholson, B. Sicardy, S. Lemouelic, S. Rodriguez, K. Stephan, C. K. Scholz, "Release of volatiles from a possible cryovolcano from near-infrared imaging of Titan," *Nature*, 435(7043) 786-789 (2005).
- 51 A. Coustenis and M. Hirtzig, "Cassini-Huygens results on Titans surface," *Research in Astronomy and Astrophysics*, 9(3):249-268 (2009).
- 52 R. D. Lorenz, "Thermodynamics of geysers: Application to Titan," *Icarus*, 156, 176-183 (2002).
- 53 R. L. Kirk, L. A. Soderblom and R. H. Brown, "Subsurface energy storage and transport for solar-powered geysers on Triton," *Science*, 250, 424-429 (1990).
- 54 T. G. Leighton, P. R. White and D. C. Finfer, "The sounds of seas in space," *Proceedings of the International Conference on Underwater Acoustic Measurements, Technologies and Results, Heraklion, Crete, 28 June-1 July 2005, II*, 833-840 (2005).

- 
- 55 ISO 1683:2015 Acoustics -- Preferred reference values for acoustical and vibratory levels (International Organization for Standardization, Geneva, Switzerland, 2015).
- 56 T. G. Leighton, "What is ultrasound?" *Progress in Biophysics and Molecular Biology*, **93**(1-3), 383 (2007).
- 57 A. Petculescu, "A tool to corroborate lightning and a first step toward a Titanian sound scape," (2010) <http://acoustics.org/pressroom/httpdocs/159th/petculescu.htm> (last accessed: 10 January 2016).
- 58 A. Petculescu and P. Achi, "A model for the vertical sound speed and absorption profiles in Titan's atmosphere based on Cassini-Huygens data," *J. Acoust. Soc. Am.* 131, 3671 (2012) <http://dx.doi.org/10.1121/1.3699217>.
- 59 C. S. Hill and A. Petculescu, "Gasdynamic modeling of strong shock wave generation from lightning in Titan's troposphere," *J. Acoust. Soc. Am.* 129, 2411 (2011) (doi:10.1121/1.358786).
- 60 A. D. Hanford and L. N. Long, "The direct simulation of acoustics on Earth, Mars and Titan," *J. Acoust. Soc. Am.*, 125(2), 640-650 (2009) (doi: 10.1121/1.3050279).
- 61 A. J. Abdullah, "The "musical" sound emitted by a tornado," *Monthly Weather Review*, 94(4), 213-220 (1966).
- 62 M. J. Lighthill, "On sound generated aerodynamically. I. General theory," *Proc. R. Soc. Lond. A* 222, 564–587 (1952) (doi:10.1098/rspa.1952.0060)
- 63 C. L. Morfey, "Amplification of aerodynamic noise by convected flow inhomogeneities," *J. Sound and Vibration*, 31, 391-397 (1973).
- 64 H. E. Bass and J. P. Chambers, "Absorption of sound in Martian atmosphere," *J. Acoustical Society of America*, 109(6), 3069-3071 (2001).
- 65 J-P. Williams, "Acoustic environment of the Martian surface," *J. Geophysical Research*, 106(E3), 5033-5041 (2001).
- 66 Y. Drain, R. M. Lueptow, "Acoustic attenuation in three-component gas mixtures – Theory," *J. Acoustical Society of America*, 109, 1955-1964 (2001).
- 67 Y. Z. Zhao, Z. I. Gu, Y. Z. Yu, Y. Ge, Y. Li, X. Feng, "Mechanism and large eddy simulation of dust devils," *Atmosphere-Ocean*, 42(1), 61-84 (2004).
- 68 M. Blame, R. Greeley, "Dust devils on Earth and Mars," *Reviews of Geophysics*, 44, RG3003 (2006).
- 69 T. L. Jackson, W. M. Farrell, G. T. Delory and J. Nithianandam, "Martian dust devil electron avalanche process and associated electrochemistry," *J. Geophysical Research*, 115, E05006 (2010).
- 70 Z. Gu, Y. Zhao, Y. Li, Y. Yu, X. Feng, "Numerical simulation of dust lifting within dust devils - simulation of an intense vortex," *J. Atmospheric Sciences*, 63, 2630-2641 (2006).

- 
- 71 J. O. Hinze, Turbulence McGraw-Hill series in mechanical engineering, 1975
- 72 N. Saptadji and D.H. Freeston. "Laboratory model of geysers: some preliminary results." Proc 13th Zealand Geothermal Workshop (1991) pp. 155-160.
- 73 S. Lasic, "Geyser model with real-time data collection," *European Journal of Physics*, 27, 9951005 (2006).
- 74 X. Lu and A. Watson, "A Review of Progress in Understanding Geysers," Proceedings World Geothermal Congress 2005 (Antalya, Turkey, 24-29 April 2005) 6 pages.
- 75 E. Adelstein, A. Tran, C. Muñoz Saez, A. Shteinberg, M. Manga, "Geyser preplay and eruption in a laboratory model with a bubble trap," *Journal of Volcanology and Geothermal Research* 285, 129–135 (2014).
- 76 Lorenz R. D., "Thermodynamics of Geysers: Application to Titan," *Icarus* 156, 176–183 (2002) doi:10.1006/icar.2001.6779.
- 77 B. Berges, "The creation of extraterrestrial soundscapes by simulating the sounds of other worlds," MSc Thesis for University of Southampton (2011) 99 pages.
- 78 N. M. Saptadji. Modeling of geysers. PhD thesis, Department of Engineering science, School of Engineering, University of Auckland, New Zealand, 1995 (403 pages).
- 79 T. G. Leighton, P. R. White and M. A. Marsden, "The one-dimensional bubble: An unusual oscillator, with applications to human bioeffects of underwater sound," *European Journal of Physics*, **16**, 275-281 (1995).
- 80 T. G. Leighton, P. R. White and M. A. Marsden, "Applications of one-dimensional bubbles to lithotripsy, and to diver response to low frequency sound," *Acta Acustica*, **3**(6), 517-529 (1995).
- 81 T. G. Leighton, "The inertial terms in equations of motion for bubbles in tubular vessels or between plates," *Journal of the Acoustical Society of America*, **130**(5), 3333-3338 (2011) (doi: 10.1121/1.3638132)
- 82 M. N. Banda, "Acoustics of natural phenomena on other planets and satellites" MSc thesis, University of Southampton (2011) 93 pages.
- 83 W. H. Bragg, Sir, "The World of Sound," (G. Bell and Sons Ltd., London) 196 pages (1921).
- 84 A. M. Worthington, "A Study of Splashes" (Longmans, Green, and Company, London) 129 pages, (1908).
- 85 University of Southampton, "The world's first planetarium show featuring the sounds and voices of other worlds," [http://www.southampton.ac.uk/engineering/research/projects/media/sound\\_in\\_space/worlds\\_first\\_planetarium\\_show.page](http://www.southampton.ac.uk/engineering/research/projects/media/sound_in_space/worlds_first_planetarium_show.page) (2012) (date last viewed 31/01/16).

- 
- 86 University of Southampton, “Southampton software used in the 19th Dutch Annual Quiz,” [http://www.southampton.ac.uk/engineering/research/projects/media/sound\\_in\\_space/19th\\_dutch\\_annual\\_quiz.page](http://www.southampton.ac.uk/engineering/research/projects/media/sound_in_space/19th_dutch_annual_quiz.page) (2012) (date last viewed 31/01/16).
- 87 University of Southampton, “BBC's The Sky At Night features voice changer,” [http://www.southampton.ac.uk/engineering/research/projects/media/sound\\_in\\_space/bbc\\_the\\_sky\\_at\\_night.page](http://www.southampton.ac.uk/engineering/research/projects/media/sound_in_space/bbc_the_sky_at_night.page) (2014) (date last viewed 31/01/16).

## FIGURE CAPTIONS

- Figure 1. (Color online) (a) A computer reconstruction of the surface of Venus, created from data from the Magellan spacecraft. Credit: E. De Jong et al. (JPL), MIPL, Magellan Team, NASA <http://www.space.com/18525-venus-composition.html> (b) Dust devil recorded by the HiRISE camera on board the Mars Reconnaissance Orbiter. Tracking across the flat, dust-covered Amazonis Planitia in the northern Martian spring of 2012, the core was about 140 meters in diameter. Lofting dust into the thin Martian atmosphere, its plume reaches about 20 kilometers above the surface. Tangential wind speeds of up to 110 kilometers per hour are reported for dust devils in other HiRISE images. Image Credit: HiRISE, MRO, LPL (U. Arizona), NASA.<http://apod.nasa.gov/apod/ap150303.html>. (c) False colour image of evidence for a possible cryo-volcano on Titan, photo credit, NASA, Cook *et al.* [30].
- Figure 2. (Color online) (a) Simulated lightning bolt generated using segment lengths of 3 cm in random alignment, showing two different lightning strikes that impact the same point on the ground. (b) Thunder model as a linear superposition of N-wave generating from lightning bolt segments.
- Figure 3. (a) Sketch of the numerical model geometry for calculating the sound from the dust devil. (b) The scaling of flow velocity profiles (vertical, tangential and radial) as a function of altitude for Martian dust devil calculations.
- Figure 4. The profiles, as a function of vertical lifting velocity, of the particle diameter (black, left) and bulk density (grey, right) profiles.
- Figure 5. Schematics of the two experimental arrangements used for the geyser/cryo-volcano.
- Figure 6. The greyscale plots the intensity on a time-frequency map for the predicted sound received on flat ground 1 km from the point where the lightning strike shown in Fig. 2 strikes the ground, for Earth, Mars, Venus and Titan. No refraction or ground effects are included, and the artificial assumption is made that the lightning produces the same acoustic intensity at source, such that the dB levels (plotted re  $1 \text{ pW m}^{-2}$ ) only reflect the effect of atmospheric absorption (there is no absorption included for Earth).

Figure 7. (Color online) Simulated rms acoustic pressure from a Martian dust devil at (a) 500 Hz, (b) 2000 Hz, (c) 3500 Hz and (d) 5000 Hz.

Figure 8. (Color online) Simultaneous plots of (a) the change in volume in the upper lake during an eruption (the starting temperature at the lower reservoir was 80 Celsius) and (b) the rms acoustic pressure record from a hydrophone in the lake in the upper flask (which at times was exposed to air – see text).

Figure 9. Time histories of the temperature in the deep reservoir (a,c) and the lake (b,d). The first pair of simultaneous records (a,b) are recorded when the lake temperature began at just over 50 °C. The second set of simultaneous data (c,d) were recorded when the lake temperature oscillated around 78 °C. Both were ‘boiling’ eruptions. The black line in (c,d) is the temperature during one eruption cycle and the grey area represents the 25<sup>th</sup>-75<sup>th</sup> percentiles interval computed over ten consecutive eruption cycles. Concurrent with the black line temperature data in (c,d), panel (e) shows hydrophone data from the lake in the upper flask (note comments in Fig. 8), and panel (f) shows data from an accelerometer placed on the outside of the upper flask.

Figure 10 (Color online) (a) Microphone data for in-air sound during a shooting eruption, with (inset) the Welch Power Spectral Density of the data. (b,c) Transposition of that data for Titan (arbitrary dB references are used for microphone voltages).

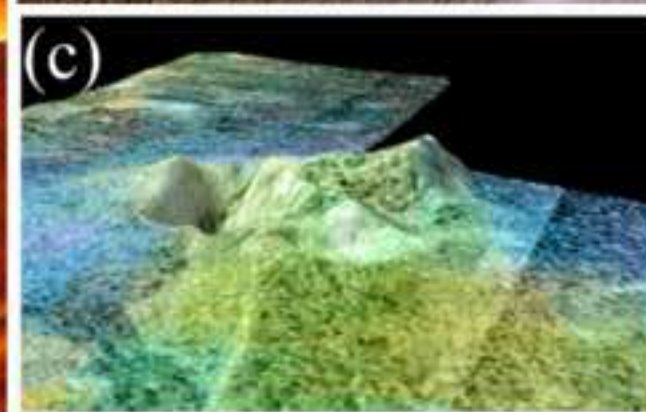
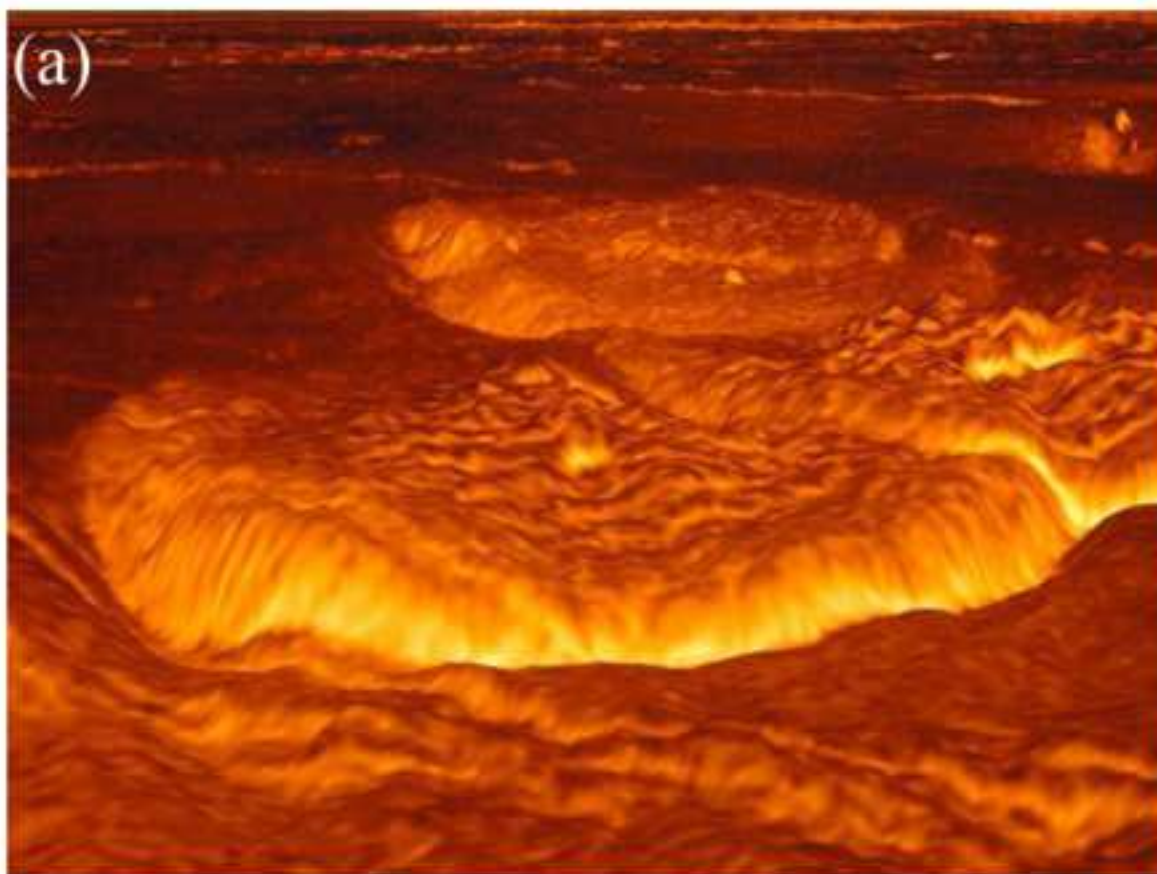
**Short (running) title:** Extraterrestrial sound for planetaria

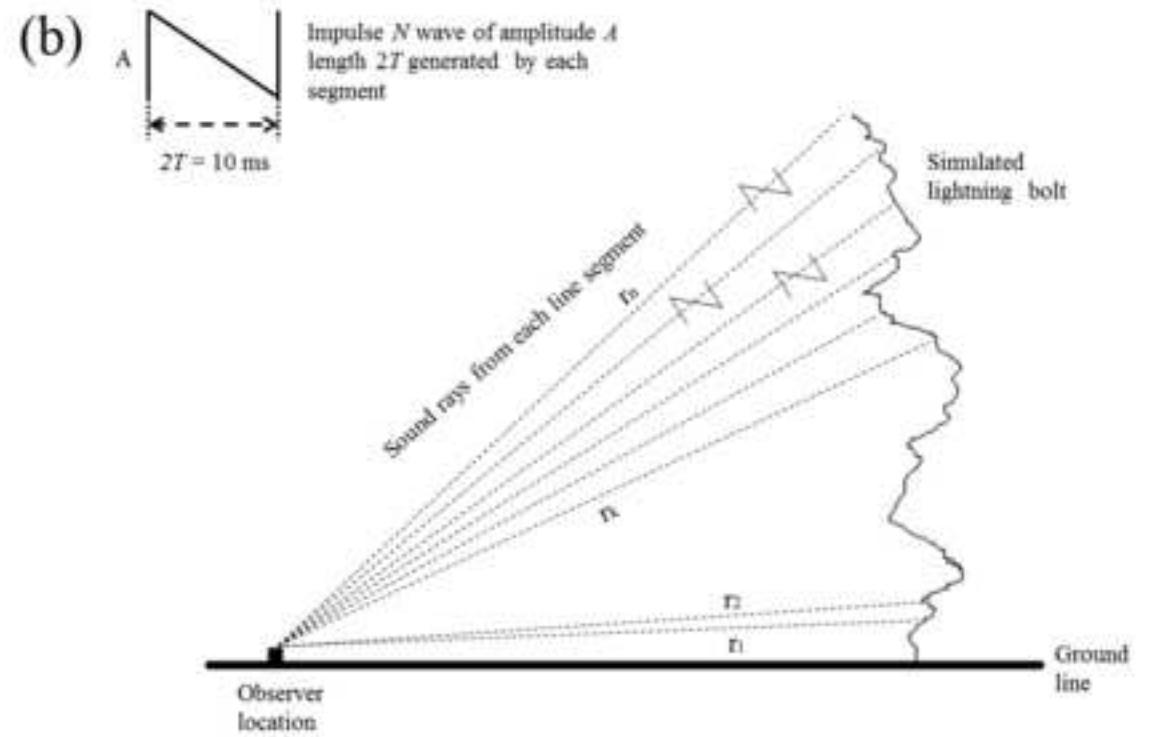
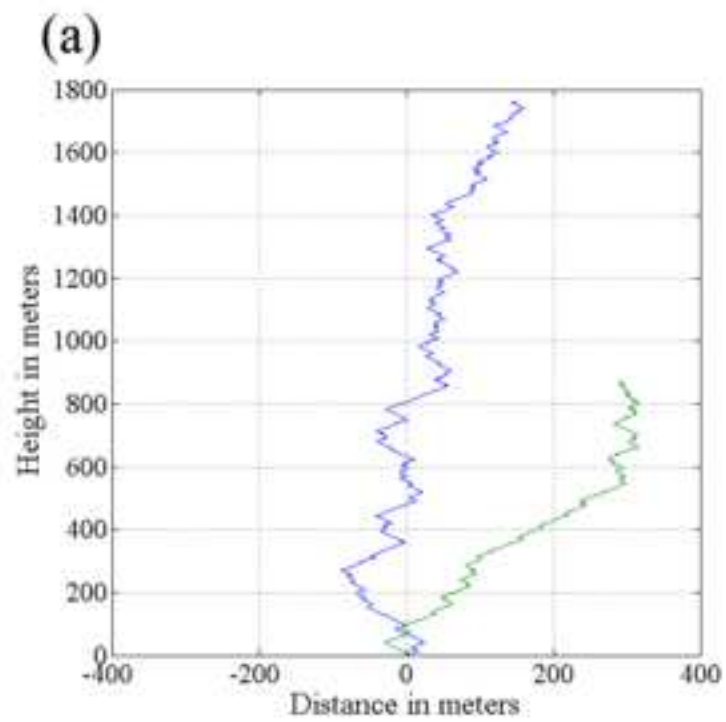


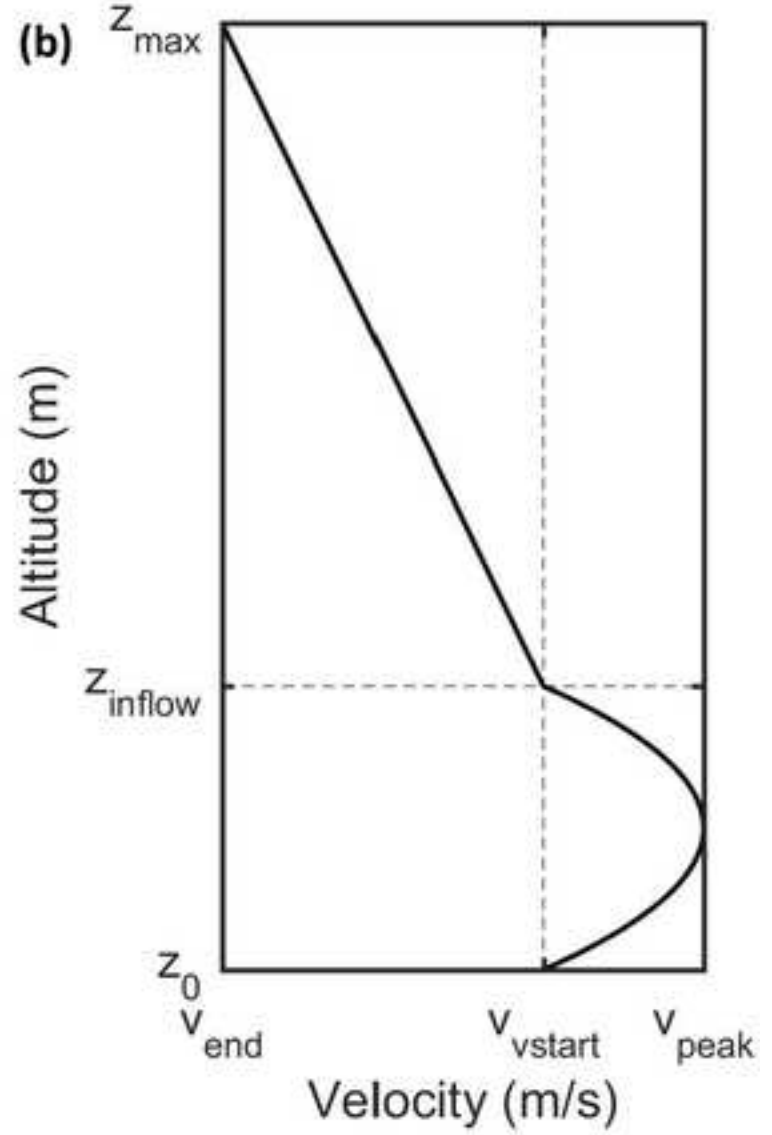
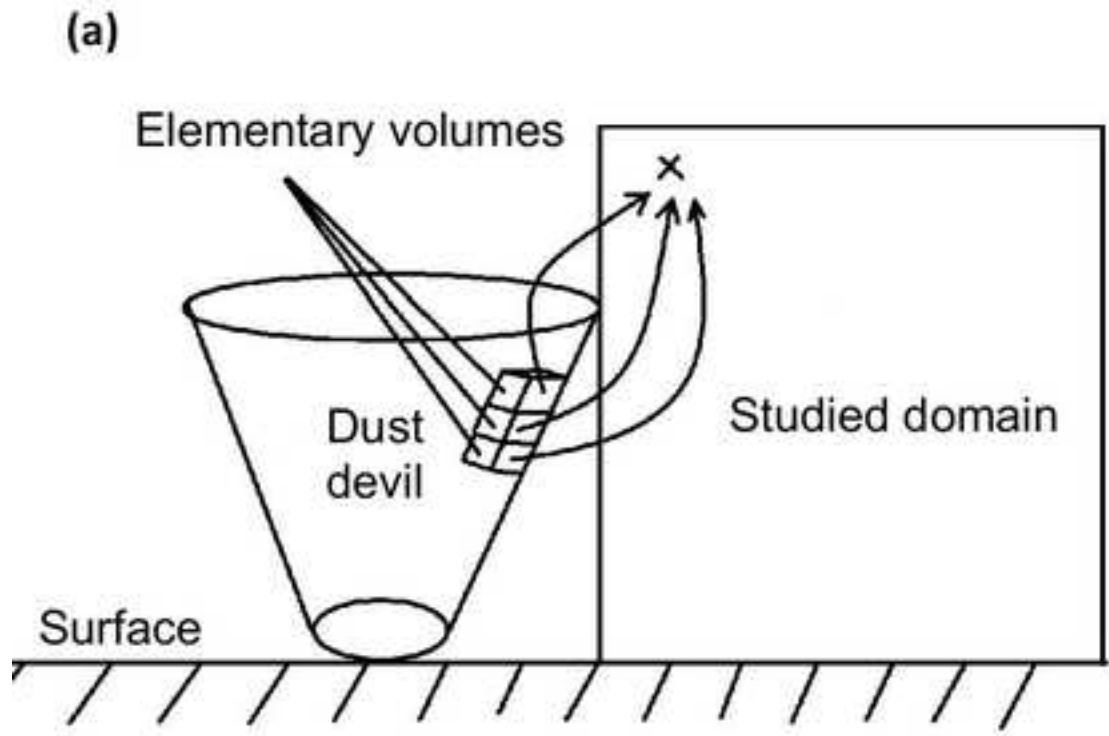
Click here to access/download

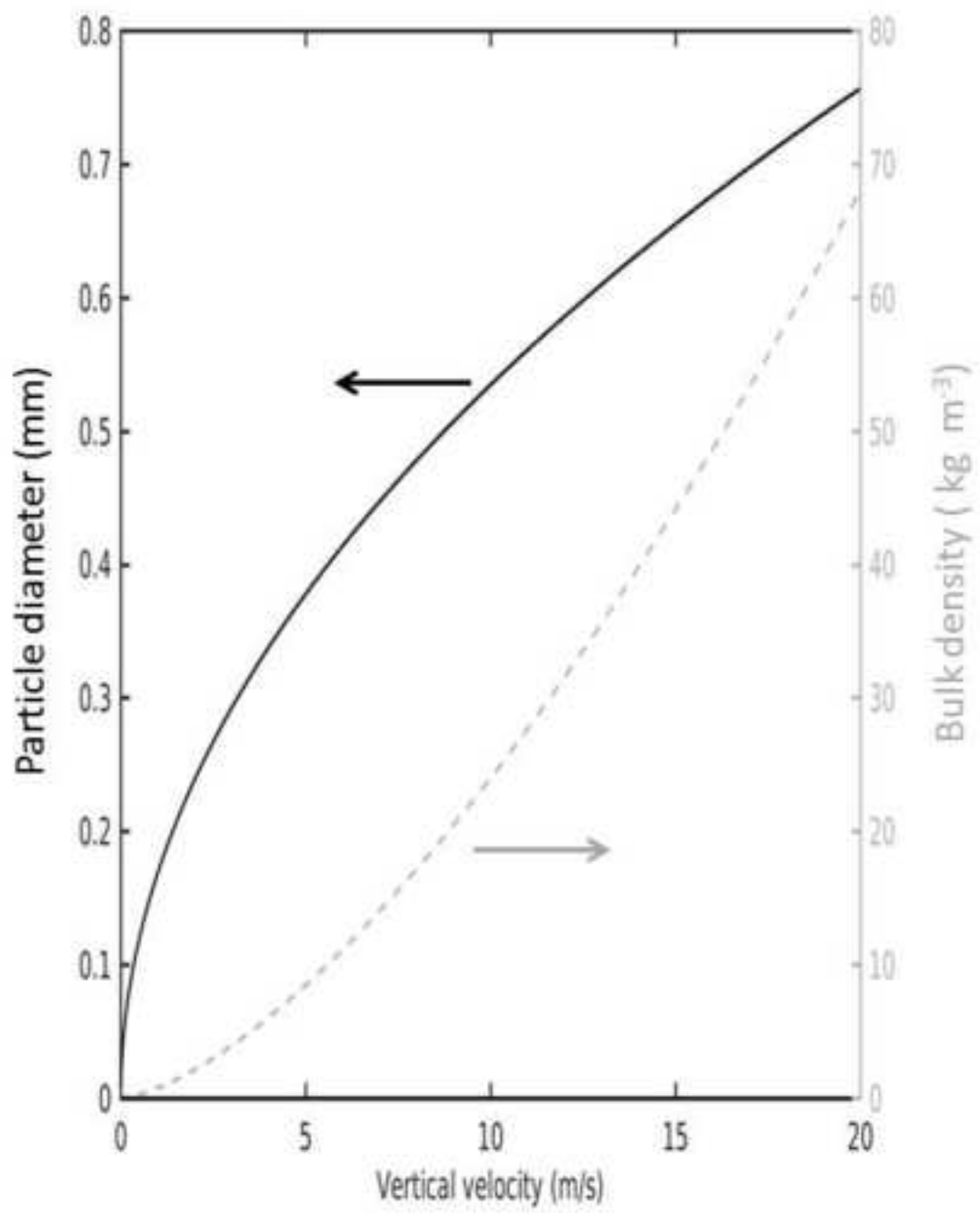
**Reviewer PDF with line numbers, inline figures and captions**

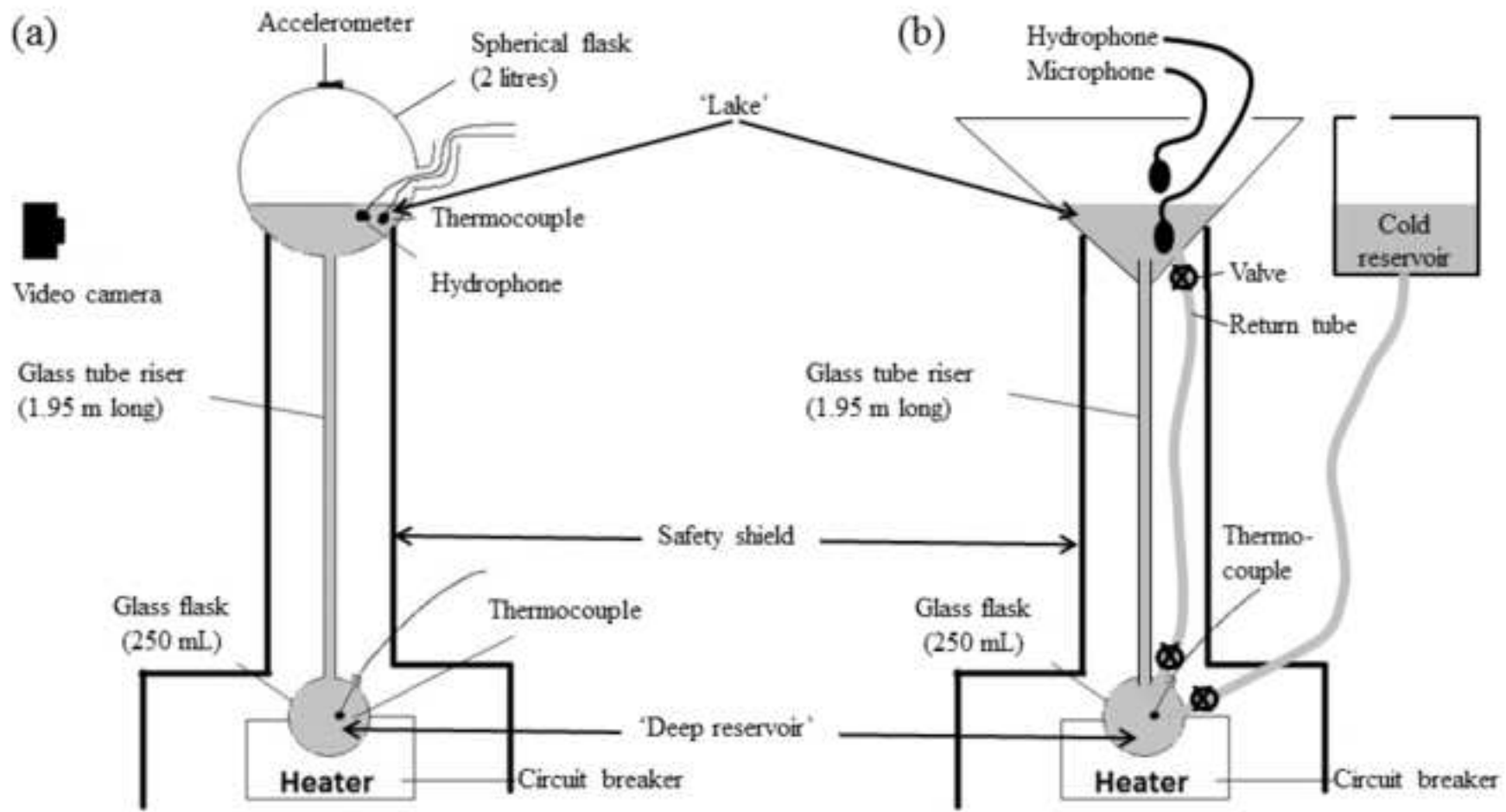
Sound for planetaria JASA v307 (for submission 22)  
(with figures).docx



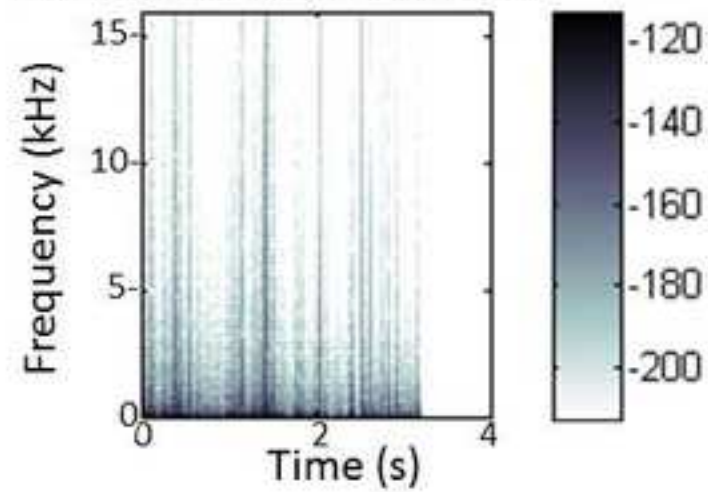




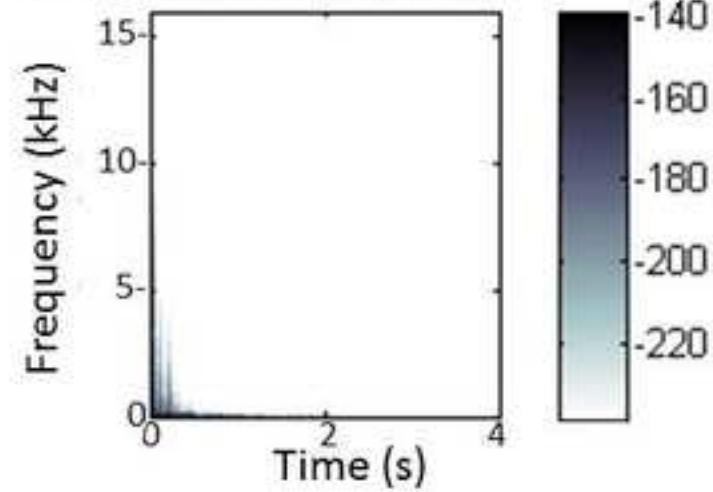




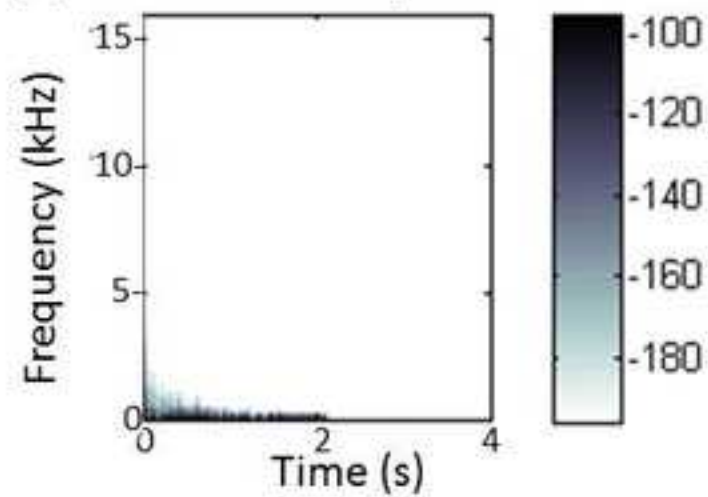
(a) Earth without absorption



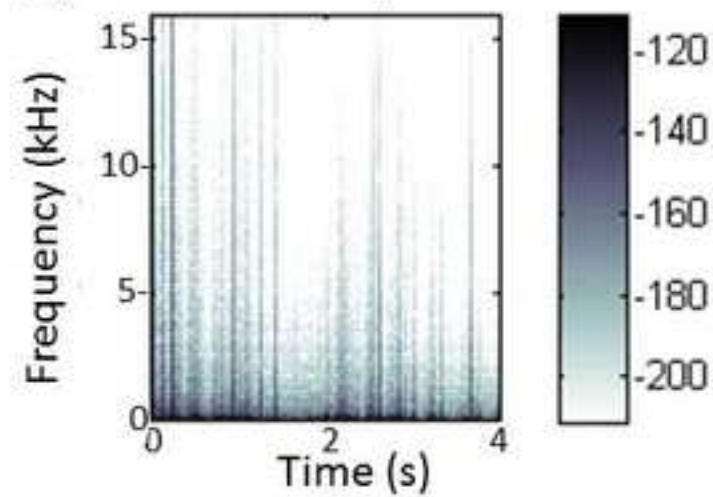
(b) Mars with absorption

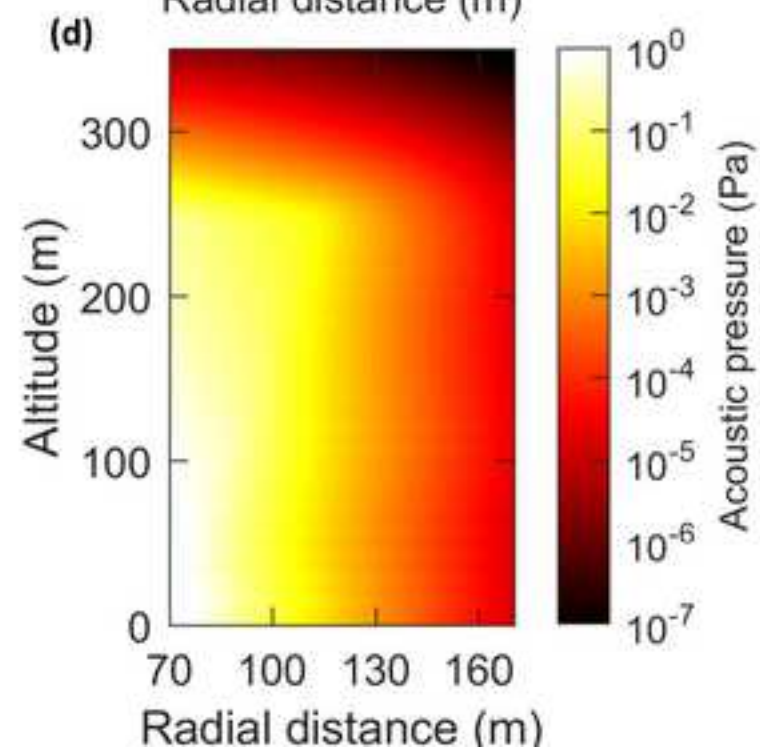
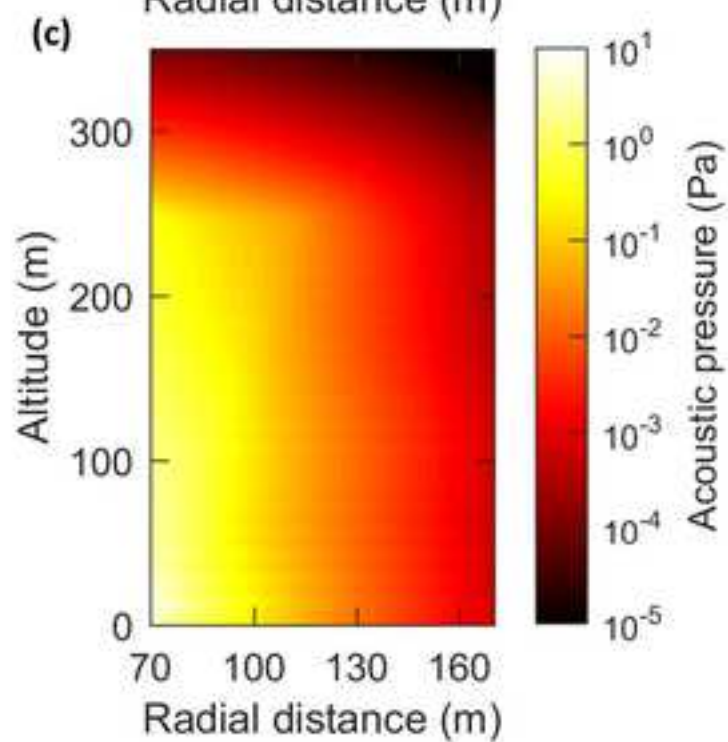
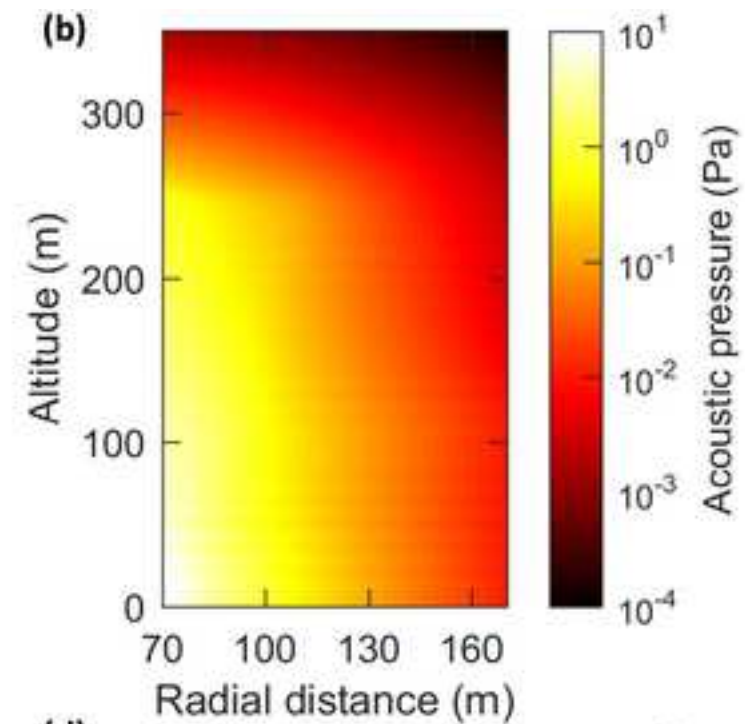
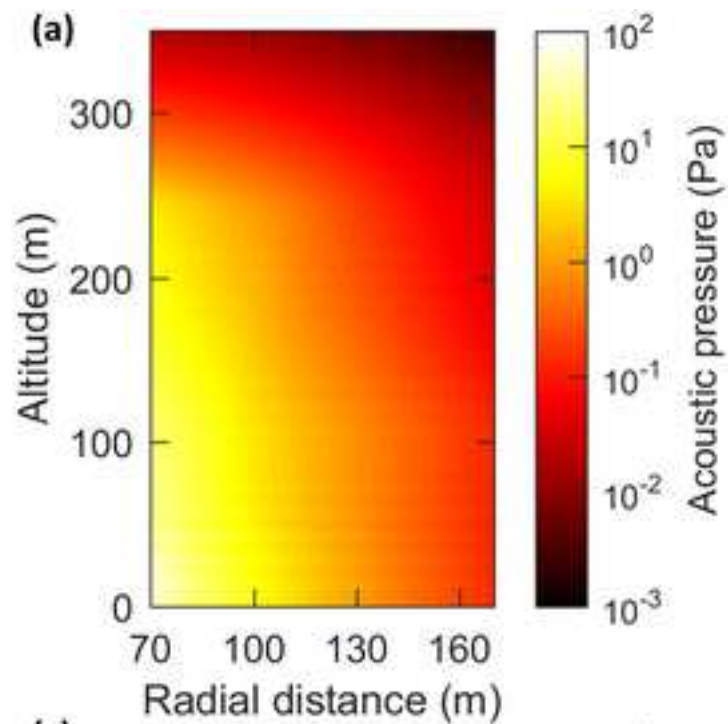


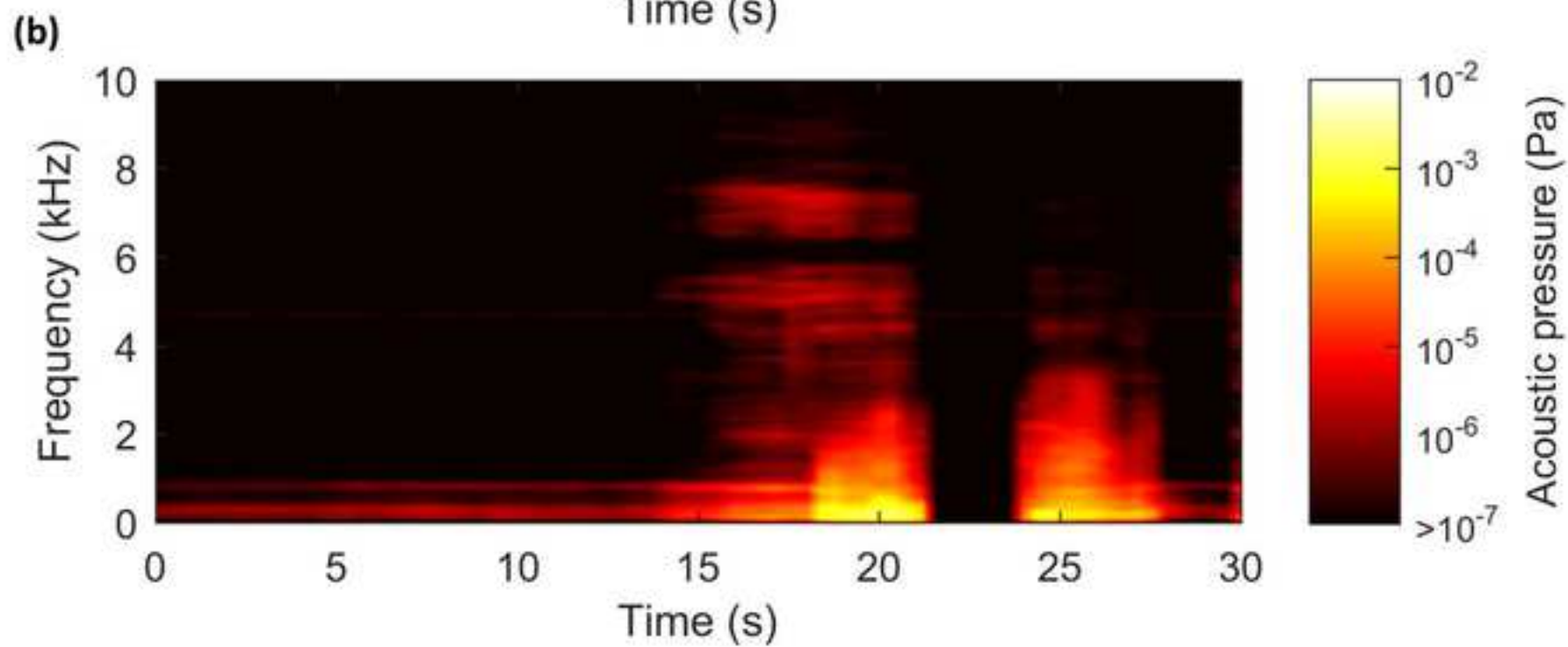
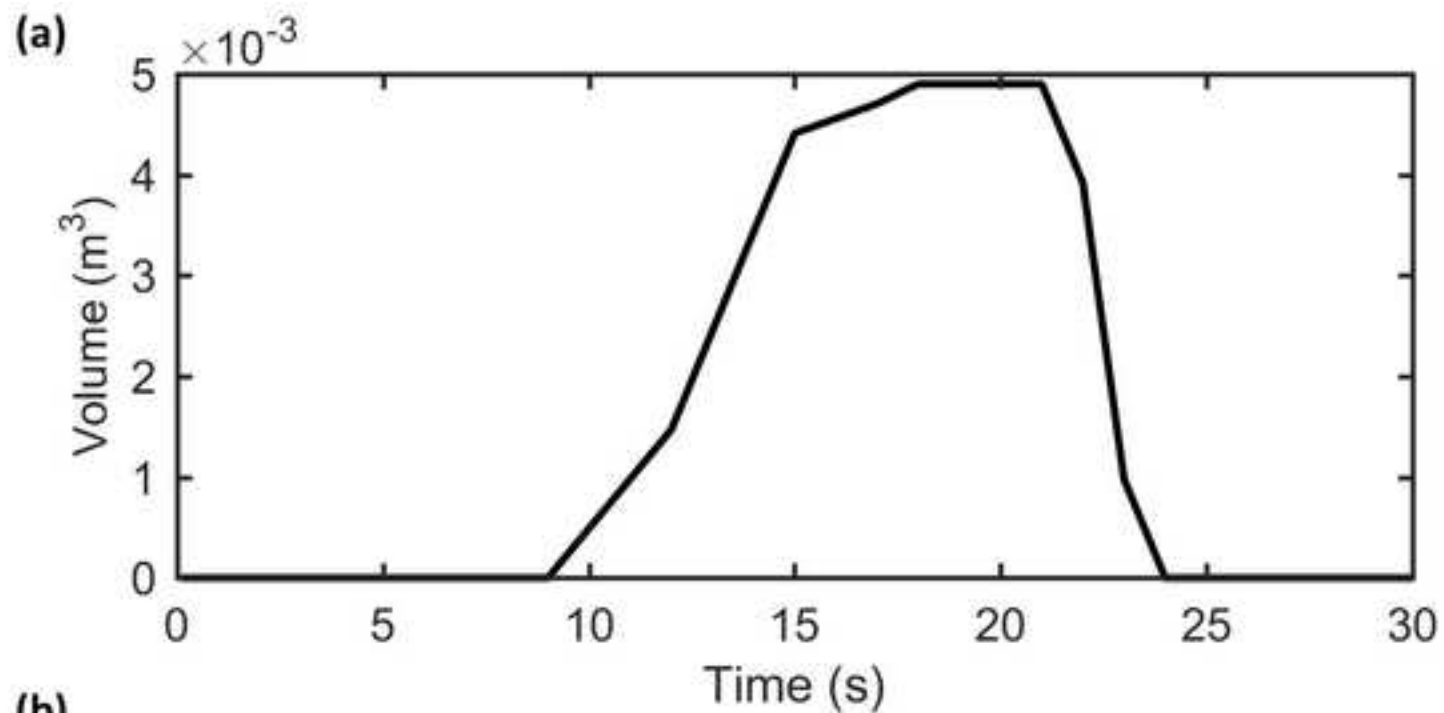
(c) Venus with absorption

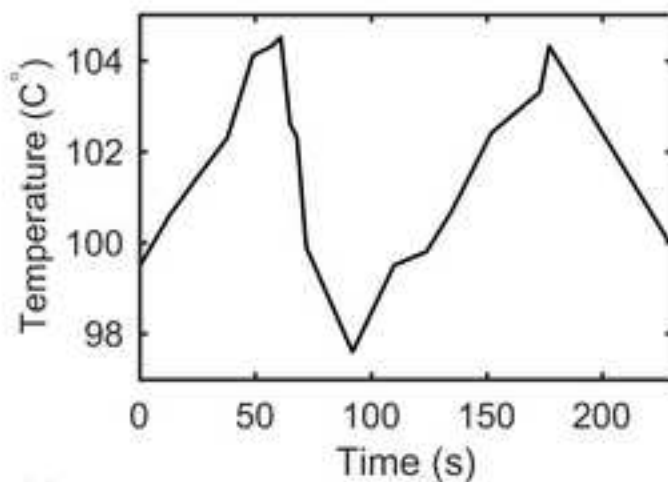
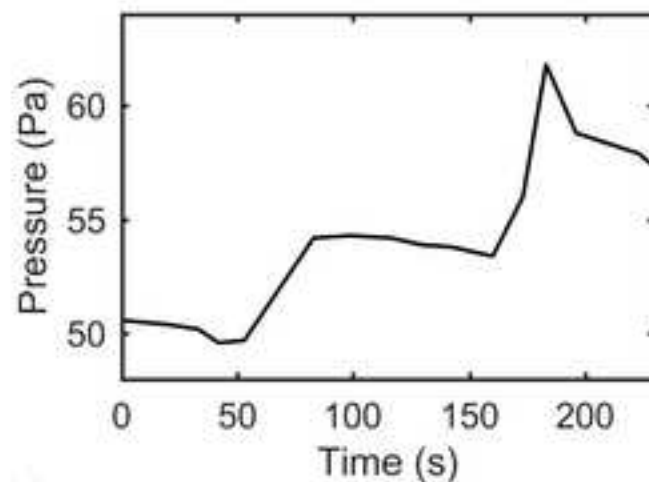
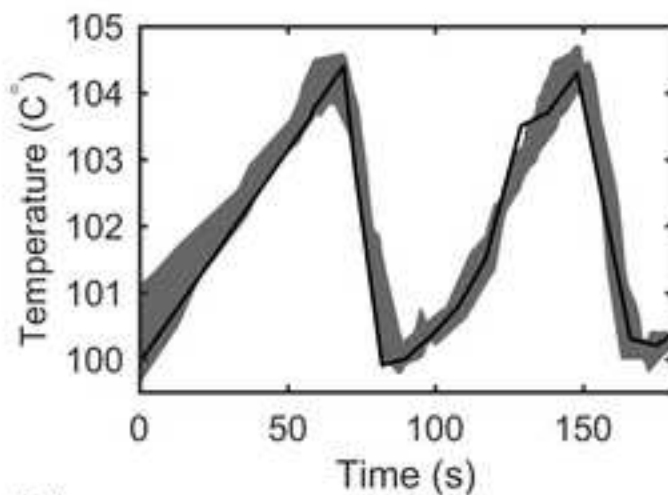
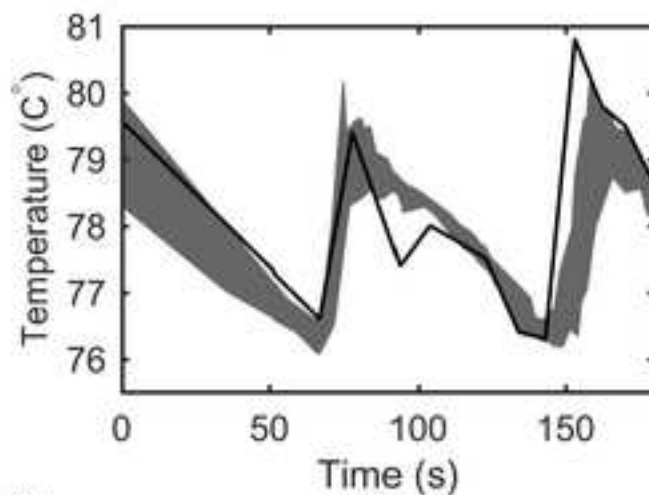
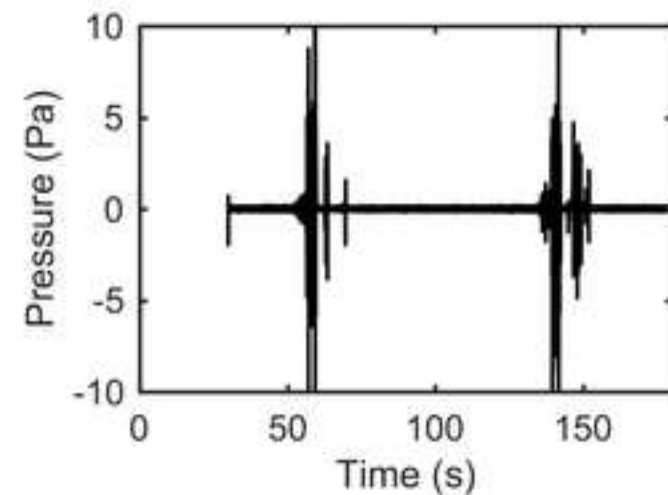


(d) Titan with absorption







**(a)** Deep reservoir temperature**(b)** Lake temperature**(c)** Deep reservoir temperature**(d)** Lake temperature**(e)** Hydrophone**(f)** Accelerometer